A COMPARATIVE STUDY OF THE COASTAL MARINE AEROSOL.

Alan Anthony Simoncic

NAVAL POSTGRADUATE SCHOOL
Monterey, California

THESIS

A COMPARATIVE STUDY OF THE

COASTAL MARINE AEROSOL

by

Alan Anthony Simoncic

December 1977

Thesis Advisor: Kenneth L. Davidson

Approved for public release; distribution unlimited.

SECURITY CLASSIFICATION OF THIS PAGE (When Data Entered)

REPORT DOCUMENTATION PAGE

READ INSTRUCTIONS BEFORE COMPLETING FORM

1. REPORT NUMBER

2. GOVT ACCESSION NO.

3. RECIPIENT'S CATALOG NUMBER

4. TITLE (and Subtitle)
A Comparative Study of the Coastal Marine Aerosol

5. TYPE OF REPORT & PERIOD COVERED
Master's Thesis; December 1977

6. PERFORMING ORG. REPORT NUMBER

7. AUTHOR(s)
Alan Anthony Simoncic

8. CONTRACT OR GRANT NUMBER(s)

9. PERFORMING ORGANIZATION NAME AND ADDRESS
Naval Postgraduate School
Monterey, California 93940

10. PROGRAM ELEMENT, PROJECT, TASK AREA & WORK UNIT NUMBERS

11. CONTROLLING OFFICE NAME AND ADDRESS
Naval Postgraduate School
Monterey, California 93940

12. REPORT DATE
December 1977

13. NUMBER OF PAGES
111

14. MONITORING AGENCY NAME & ADDRESS(if different from Controlling Office)
Naval Postgraduate School
Monterey, California 93940

15. SECURITY CLASS. (of this report)
Unclassified

15a. DECLASSIFICATION/DOWNGRADING SCHEDULE

16. DISTRIBUTION STATEMENT (of this Report)

Approved for public release; distribution unlimited.

17. DISTRIBUTION STATEMENT (of the abstract entered in Block 20, if different from Report)

18. SUPPLEMENTARY NOTES

19. KEY WORDS (Continue on reverse side if necessary and identify by block number)

20. ABSTRACT (Continue on reverse side if necessary and identify by block number)

Aerosol size distributions near the coast of Panama City, Florida and off the Southern California coast near the Channel Islands are investigated in this study. The relationships of the coastal marine aerosol to wind speed, relative humidity, stability, and sub-synoptic circulation are examined. Relative humidity and stability are shown to have the largest effect on the aerosol distribution

DD FORM 1 JAN 73 1473 EDITION OF 1 NOV 65 IS OBSOLETE
S/N 0102-014-6601 |
(Page 1)

SECURITY CLASSIFICATION OF THIS PAGE (When Data Entered)

during periods of light winds. Coalescence and sedimentation of droplets greater than 1.5 μ radius are most pronounced when the wind speed and sea surface production of salt nuclei are weak. When wind speeds exceed 7 m/sec, a state of equilibrium between sedimentation and production of these larger droplets appears to exist. An apparent zone of transition between the two bubble bursting sea-salt producing mechanisms is observed near .5 μ radius. The highest correlation between wind speed and particle concentration occurs under unstable conditions. Secondary circulations are shown to be important determinants of the coastal marine aerosol in the absence of synoptic scale forcing.

Approved for public release; distribution unlimited.

A Comparative Study of the Coastal Marine Aerosol

by

Alan Anthony Simoncic
Captain, United States Air Force
B.S., United States Air Force Academy, 1970

Submitted in partial fulfillment of the
requirements for the degree of

MASTER OF SCIENCE IN METEOROLOGY

from the

NAVAL POSTGRADUATE SCHOOL
December 1977

ABSTRACT

Aerosol size distributions near the coast of Panama City, Florida and off the Southern California coast near the Channel Islands are investigated in this study. The relationships of the coastal marine aerosol to wind speed, relative humidity, stability, and sub-synoptic circulation are examined. Relative humidity and stability are shown to have the largest effect on the aerosol distribution during periods of light winds. Coalescence and sedimentation of droplets greater than 1.5 μ radius are most pronounced when the wind speed and sea surface production of salt nuclei are weak. When wind speeds exceed 7 m/sec, a state of equilibrium between sedimentation and production of these larger droplets appears to exist. An apparent zone of transition between the two bubble bursting sea-salt producing mechanisms is observed near .5 μ radius. The highest correlation between wind speed and particle concentration occurs under unstable conditions. Secondary circulations are shown to be important determinants of the coastal marine aerosol in the absence of synoptic scale forcing.

TABLE OF CONTENTS

LIST OF TABLES

LIST OF FIGURES

ACKNOWLEDGEMENTS

Appreciation and thanks are extended to Dr. Kenneth L. Davidson for his support and guidance throughout this study. Dr. Chris Fairall and Dr. Gordon Schacher aided immeasurably by offering technical assistance and advice. Many thanks also to Mr. Gene Mack for providing the aerosol and meteorological data used in this investigation.

A special and heartfelt appreciation must go to my wife, Sue, and sons, David and Adam, for their constant expression of encouragement and understanding.

I. INTRODUCTION

The military is currently very interested in the performance of electro-optical weapons systems in an atmosphere of varying turbidity. For example, a number of electro-optical systems which utilize the visible as well as IR wavelengths are being developed by the Navy for use in surveillance and intelligence gathering operations in the marine boundary layer. These systems are limited by the extinction of the propagated energy due to absorption and scattering by aerosols. The effect of absorption depends on the composition of the particulates and wavelength of the energy and the effect of scattering depends on the concentration and size of the scatterers. For most applications the scattering processes in the atmosphere are caused by particles of size comparable to the wavelength of the radiation.

The size distribution of the marine aerosol is known to depend upon the wind speed, relative humidity, stability, and air mass trajectory. In order to evaluate accurately and predict the atmospheric effects on these electro-optic systems, it is necessary to know the dependence of the aerosol size distribution on the foregoing meteorological parameters.

The nature of the aerosol size distribution in a coastal marine environment is investigated in this study. Data from aerosol observations off the coast of Panama City, Florida and off the Southern California coast near the Channel Islands

were analyzed. These coastal regimes, which represent a mixture of continental and marine aerosols, should contain aerosol distributions somewhat different from the typical marine environment. The relationship of the coastal marine aerosol to wind speed, relative humidity, stability, and sub-synoptic circulation is examined. Furthermore, an attempt is made to evaluate the use of the friction velocity as a valid aerosol distribution predictor.

II. BACKGROUND

A. THE ATMOSPHERIC AEROSOL

With the recent increasing concern over the pollution of our atmospheric environment, the examination of the tropospheric aerosols has also increased. Particulate matter enters the atmosphere through either natural or man-made processes; approximately 10% of the total concentration is believed to originate from combustion and industrial processes while the natural sources, including soil dust, volcanoes, and oceans account for the remaining 90%. The size range of aerosols observed by current methods extends from 10^{-3} μ to 10^{3} μ radius (1 μ = 10^{-6}m = micron). Depending on their size, amount of soluble matter, and the relative humidity, these particles may act as condensation nuclei and aid in the precipitation process.

Mason (1975) classified condensation nuclei into three groups according to radius: Aitken (< 0.1 μ), Large (0.1 μ - 1 μ), and Giant (> 1 μ) particles. Essentially, Aitken nuclei are produced by man-made sources and larger nuclei by natural processes. Therefore, it is not surprising to see Aitken nuclei dominate the size distribution spectrum over continents. The marine aerosol above .1 μ is composed of sea-salt particles produced by spray and bubble bursting mechanisms on the water surface. These mechanisms are quite complex and their contribution to the size distribution will be discussed in detail later.

The vertical profiles of trace constituents that are produced over the continents have been shown to be rather uniform in space and time above 5 km. This "background" aerosol is affected slightly by anthropogenic activities and is far away from local natural sources. Its number concentration is almost identical with the concentration of Aitken nuclei over ocean areas. Past experiments have shown the concentration of the background aerosol to be about 300 cm^{-3} over remote ocean areas. However, a recent experimental cruise (R/V Meteor) by Junge and Jaenicke, 1971 in the mid Atlantic yielded observed concentrations of 600 cm^{-3}. Measurements by Hidy, et al. (1973) on San Nicolas Island, 130 km, west-southwest of Los Angeles, have shown the background aerosol to be a mixture of material from both marine and continental sources with an average concentration of 2400 cm^{-3}. Samples taken over oceans of the South Atlantic (Meszaros and Vissy, 1974) resulted in Aitken particle counts of between 300-450 cm^{-3}.

B. CHARACTERISTICS OF THE MARINE AEROSOL

An idealized size distribution of the continental and marine aerosol is supplied by Junge (1972) in Figure 1. The significant feature is the shift of the maximum of particles as a function of total particle concentration. Over the ocean the sea-salt aerosol, which is usually confined to the lower 2 km, is superimposed on the background aerosol. Junge reasoned that the concentration of the background

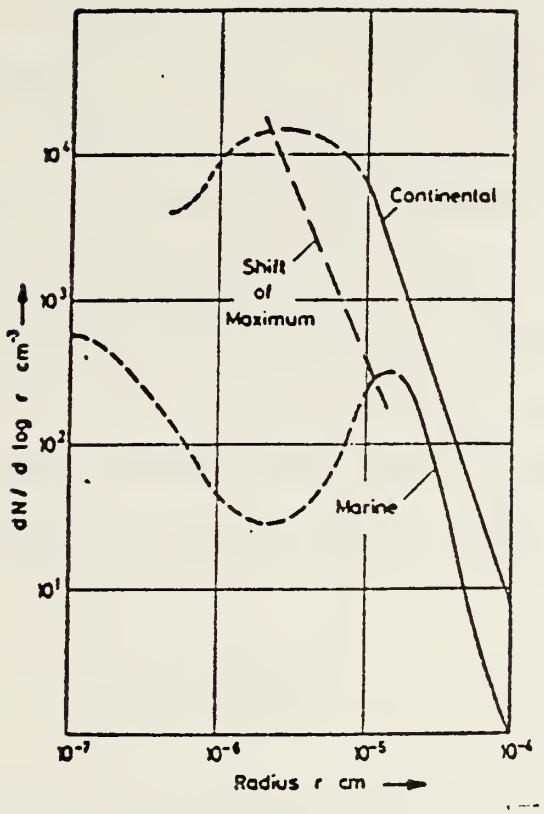

Figure 1. Idealized Size Distributions of Continental and Marine Aerosols

cloud nuclei decreases below the marine inversion due to the effect of washout, or coalescence, due to the larger water droplets in the cumulus clouds.

Another aspect of the aerosol distribution is the slope of the number density versus radius curve. Friedlander (1961) proposed a theory of self-preserving size distributions which helps to explain why all atmospheric size distributions are similar. He proposed that the similarities can be explained by solutions to the kinetic equation which describe the relationship between particle size distribution and time. Experimental results have indicated that the size distribution over a particular range of sizes of continental aerosol has a -4 slope and follows the relation

$$\frac{dN}{dr} = C\phi\, r^{-4} \qquad (1)$$

where N is the number of particles/cm^3, r the particle radius, C a constant, and ϕ the volume of particles per unit volume of aerosol.

Blifford (1970) measured the size and number distributions of atmospheric aerosols at various altitudes over the ocean 250 km west of Santa Barbara, California. Samples were taken by an aircraft equipped with a jet impactor and the data was obtained from direct microscopic counting techniques in the laboratory. The aerosol distribution at approximately 15 meters above the sea surface is presented in Figure 2. The curve has a rather steep negative slope at

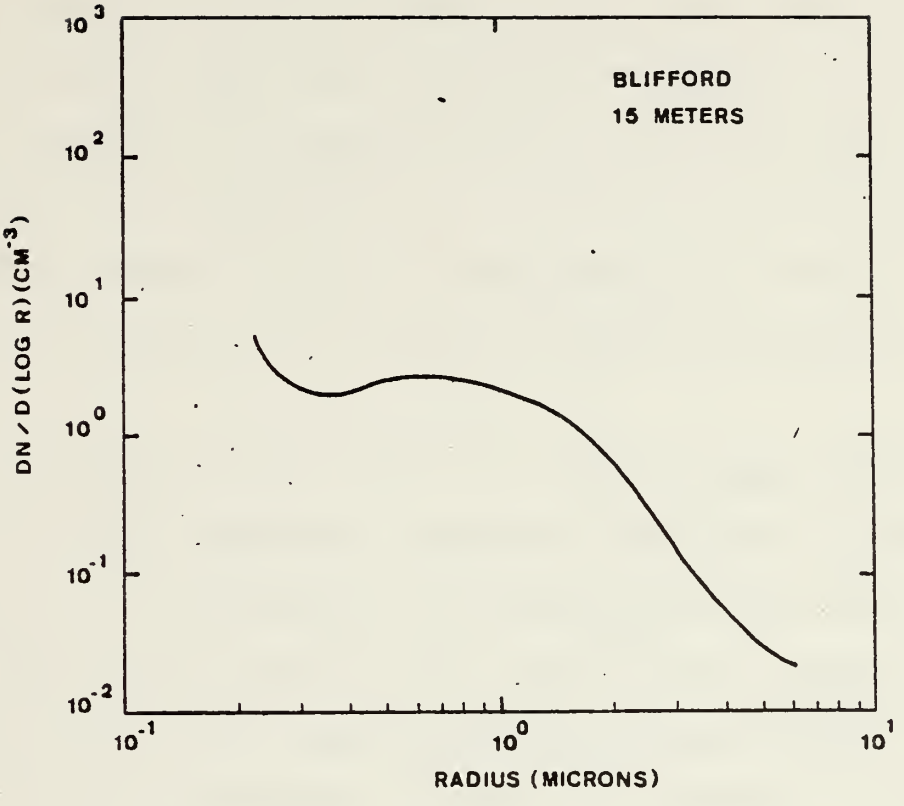

Figure 2. Size Distribution at 15 Meters, 250 km West of Santa Barbara

the small particle end which becomes slightly positive at around .4 μ radius. For particles larger than .8 μ, a fairly constant slope of about -2 to -3 is observed.

The results of the R/V Meteor experiment, where several aerosol counters were used, are shown in Figure 3. Above 10 μ the exponent of a power function fit to the data is approximately -6 and between 0.3 μ and 10 μ it is variable but on the average around -3. The maximum of the size distribution occurred at 0.3 μ with a secondary maximum at 0.03 μ.

It is possible that, due to increased human activity in the Northern Hemisphere, Junge and Jaenicke's Atlantic experiment did not explore the undisturbed marine environment. Meszaros and Vissy (1974) describe the results of aerosol samples taken over the oceans of the Southern Hemisphere by means of membrane filters. An example of the number concentration and size distribution over the Atlantic between (a) 0° and 20° South and (b) 40° and 60° South can be found in Figure 4. Chemical analyses were performed and it was observed that the maxima in the concentrations of all particles and of sodium chloride particles occur at approximately .1 μ radius in both cases. Up to .5 μ radius the slope of the distribution is approximately -5. Between 0.5 μ and 1.5 μ, however, the decrease of the concentration with increasing particle size is very moderate (-1 to -2), while for radii larger than 1.5 μ the slope is close to -3. This has been interpreted to indicate that the form of the

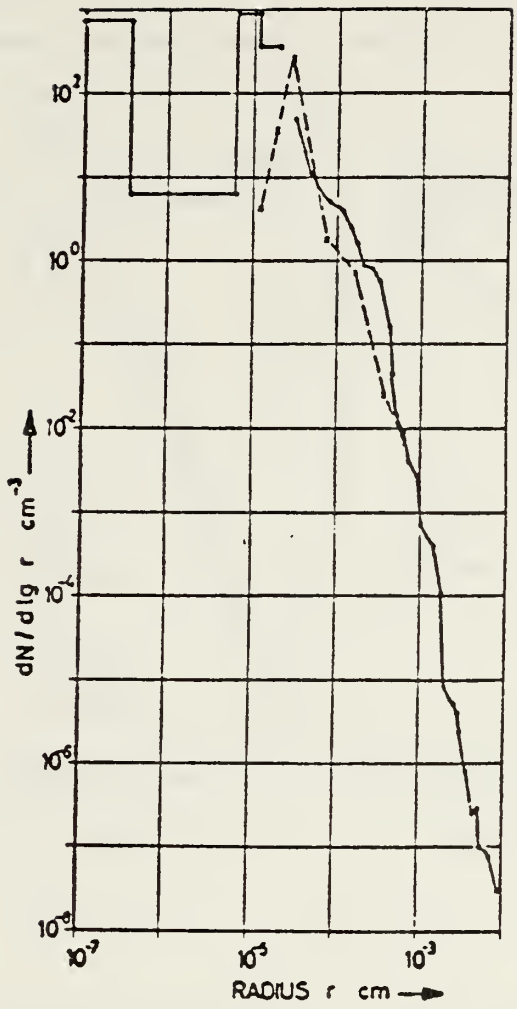

Figure 3. Results of the R/V Meter Cruise. Measurement Systems Used: o—o Combination of CCN Counter, Optical Counter, and Impactors: – – – Double Stage Impactor (Junge and Jaenicke, 1971)

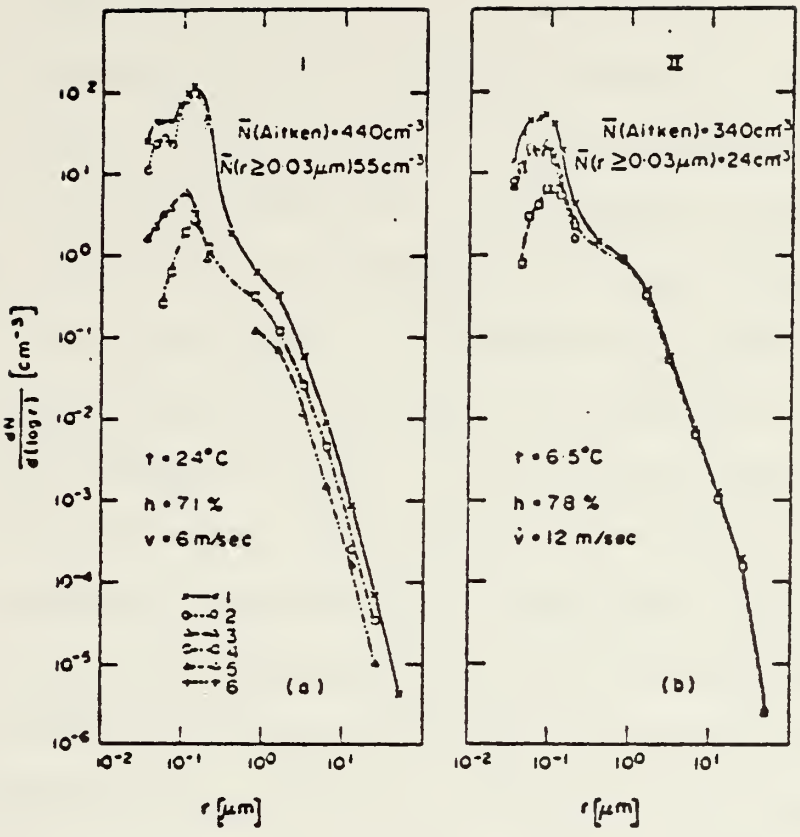

Figure 4. Size Distributions over Remote Ocean Areas (—— All Particles; —·— NaCl Particles)

distribution is produced by the combined effect of particles formed in different ways.

Oceanic measurements have shown that the concentration of sea-salt particles decreases exponentially with height, with little variation of the size distribution. Ericksson (1959) reported that there exists a level a few hundred feet above the surface where the concentration decreases with height in periods of high wind force and increases with height in lower wind forces. He reasoned that there is little or no production of sea-salt in regions of light winds and that coagulation and fallout in the lower levels combined with horizontal transport due to vertical shear produce a maximum concentration at some upper level.

Toba (1965a and b) proposed that the average decrease in concentration with height can be explained by a combination of sedimentation, diffusion, convective processes and the humidity distribution. He suggested that the line between the aerosol vertical distribution and the process of production of sea-salt particles at the sea surface is found within the lowest layer of the atmosphere where the eddy diffusivity and relative humidity sharply change.

The distribution of eddy diffusivity near the sea surface is closely related to the wind speed. The larger the eddy diffusivity near the surface the more sea-salt particles that will be supplied. Toba considered eddy diffusivity in the form

$$D = kU_{*}(Z + Z_{o}) \qquad (2)$$

where k is the von Karman constant, Z the height above the sea surface, Z_o the roughness length, and U_* the friction velocity which is a function of the momentum transfer over the sea.

The relative humidity in the first few meters over the ocean is known to decrease rapidly with height. The particles produced near the surface in a region of high humidity grow larger and thus have a greater terminal velocity due to gravity than those at the top of this layer.

During light winds the number concentration near the sea surface increases with height. Since it results from a non-steady state, an inversion of vertical gradient of the particle concentration is most likely to be found in small particles which have a longer residence time. Ericksson (1959) computed the fall velocities for given relative humidities, salinity, and radius. During high wind periods, giant size sea-salt particles are produced at the surface and through the diffusion process are mixed throughout the atmosphere. The largest particles may fall back into the ocean due to excessive terminal velocity or be entrained in the wave crests. Smaller particles are free to rise to cloud height where coalescence with larger cloud drops and washout usually occur.

Measurements of salt nuclei greater than 10^{-14} gm over the North Atlantic by Moore and Mason (1954) revealed the existence of two distinct types of size distributions (Type I and II). The curves for the observed Type I and Type II

nuclei distributions are reproduced in Figure 5. Type I distributions were observed for wind speeds between 6-15 m/sec and were thought to be residuals of spray droplets produced by breaking waves. The presence of a discontinuity or a sharp change of slope in the Type I distribution was explained in terms of a loss of the larger nuclei by sedimentation. In strong winds, the part of the curve to the right of the discontinuity probably represents a state of equilibrium between production and loss by sedimentation. In light winds and stable conditions the slope should be steeper due to the fact that the loss by sedimentation is greater than production and larger nuclei are not easily transported vertically under stable conditions. The Type II distributions were only observed when the wind speeds were less than 7 m/sec and resembled a high concentration continental aerosol. In winds of up to 15 m/sec the measured concentrations of large sea-salt nuclei rarely exceeded 10 cm^{-3}.

The effect of stability on the concentration of atmospheric condensation nuclei was well documented by Moore (1952). He used an Aitken counter to measure the relationship between concentration of nuclei and the intensity of vertical mixing over the North Atlantic. The results indicated a decrease by as much as a factor of 4 in the number of Aitken particles near the surface on days with cumulus clouds as compared to days with stratus clouds. This would indicate that convection plays an important role, at least in the transport of smaller particles.

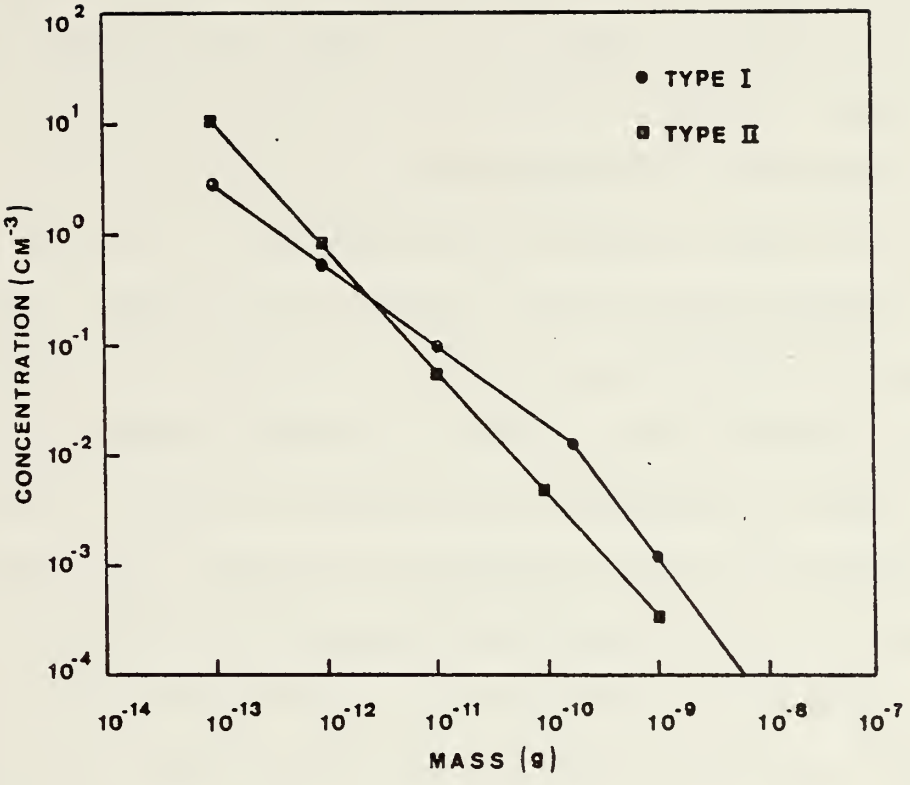

Figure 5. The Size Distribution of Moore and Mason's Type I and Type II Nuclei

Chemical analyses by various investigators have indicated that between 0.1 μ and 1.0 μ radius the marine aerosol is composed of a background component of continental origin and a sea-salt component. Sodium chloride was found to predominate above 1 μ radius while particles of continental origin predominate below 0.1 μ radius. Results of a cruise off the Grand Banks in the North Atlantic (Ruskin, et al., 1976) indicated that the continental particles are composed of sulfate compounds and a smaller amount of sulfuric acid. Aerosols over remote ocean areas (Meszaros and Vissy, 1974) were shown to be comprised of variable concentrations of ammonium sulfate, sulfuric acid, sodium chloride, and particles similar in structure to ammonium sulfate. The sum of these four types of identified particles accounted for 75-95 percent of all particles greater than .3 μ radius. In other words, practically all the particles in a pure marine atmosphere, undisturbed by continental particle sources, are soluble in water.

C. RELATIVE HUMIDITY EFFECTS

A solid particle which is composed wholly, or in part, of a pure water-soluble substance will undergo a sudden transition to a saturated solution droplet when some critical value of relative humidity, less than 100%, is reached. The relative humidity at which this transition occurs depends on the size and chemical composition of the particle. The smaller the particle, the lower the critical humidity. Below the transition point, solid particles acquire small amounts

of water by the process of adsorption. At relative humidities above the transition point, a particle (or, more properly, an aqueous solution droplet) grows by the absorption of water vapor (Fitzgerald, 1975).

A pure water droplet is said to be in equilibrium with its surroundings if it neither evaporates nor grows. This only occurs when the equilibrium vapor pressure over the surface of the droplet is equal to the vapor pressure of the surrounding air. Winkler (1973) describes the equilibrium growth of aerosol particles due to humidity as complex and depending on the relative proportion of soluble and insoluble material in the particles and on the chemical composition of the soluble component. Complex ionic mixtures, similar to those present in atmospheric aerosols, show material influences and lower the water vapor pressure to a much less degree than the same amount of pure salts. In such complex mixtures the various salts become dissolved only gradually with increasing relative humidity until at a sufficiently high humidity all soluble material is in solution.

Measurements have shown that with increasing humidity a sodium chloride crystal undergoes a phase transition to a saturated solution droplet at a relative humidity of approximately 78%. Figure 6 describes how the equilibrium radii of droplets containing specified masses of sodium chloride vary with the relative humidity. The equilibrium radius of the droplet increases with increasing humidity until the air becomes supersaturated by a critical amount, corresponding to

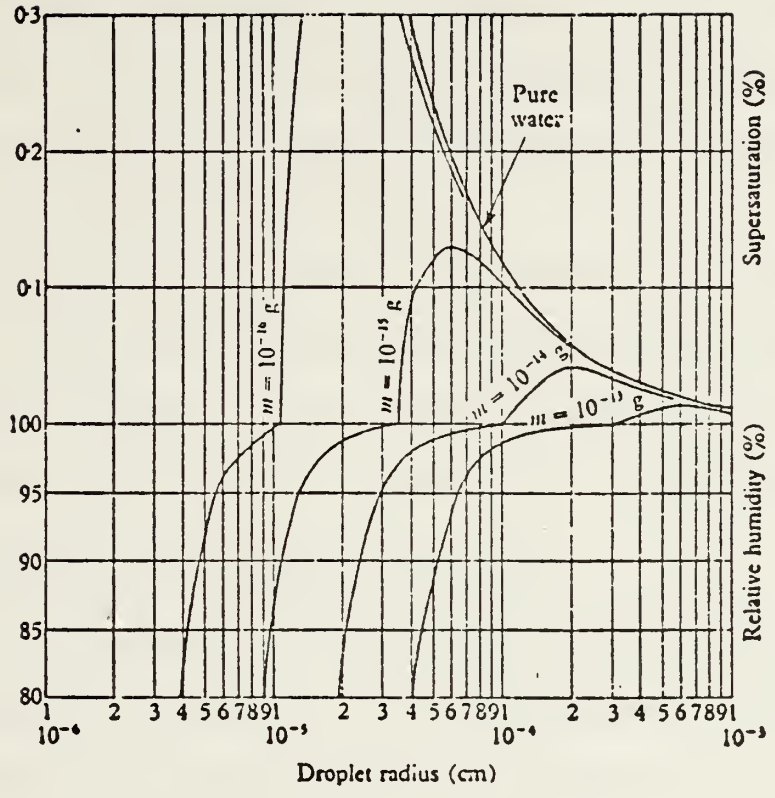

Figure 6. Equilibrium Relative Humidity and Corresponding Radii (Mason, 1975)

the maximum of the curve in this figure. If this supersaturation were maintained, theoretically the droplet will grow without bound. With decreasing humidity a sodium chloride solution droplet crystallizes at a humidity between 35-45%. Since the relative humidity at a height of about 15 meters over the ocean surface goes below 40% very infrequently, sea-salt droplets will have little opportunity to crystallize (Fitzgerald and Ruskin, 1977).

Since the later discussion refers to the distribution of sea-salt particles by bolt mass weight of salt (grams), radius of dry crystals (μ) or radius at ambient humidity (μ), the scale in figure 7 is furnished as a reference.

D. THE PRODUCTION OF AIRBORNE SEA-SALT

Although the spectrum of the marine aerosol above .1 μ radius is known to consist of sea-salt particles, very little is certain about the concentration and mechanisms of production. Because of the smallness of the particles and limitations of the sampling equipment, earlier experiments did not measure the quantity of sea-salt particles much less than 10^{-12} gm.

Woodcock (1953) determined that the mass distribution of "giant" (> 10^{-12} gm) sea-salt nuclei varies with wind speed. Increases in the amount of air-borne salt near cloud bases were shown to be related to increases in wind speed at the sea surface, with the greatest proportionate increase in particle number occurring at the large end of the weight range. The results of Woodcock's measurements for wind forces of 1,

3, 5, and 7 on the Beaufort scale are shown in Figure 7. The line (a) gives the size distribution of continental aerosol for comparison. The line (b) is an extrapolated size distribution of the marine aerosol. Chemical analysis of Woodcock's bulk aerosol samples between .1 μ and 1 μ indicated a maximum of sea-salt around 0.3 μ and a lower limit in the vicinity of .1 μ radius. These distributions indicate total concentrations of all sea-salt particles of no higher than a few per cubic centimeter (Junge, 1972). According to Mason (1975), over a rough sea the concentration of sea-salt particles greater than 2 μ radius rarely exceeds 1 cm^{-3} and the total concentration of all salt particles rarely exceeds 10 cm^{-3}.

Moore (1952) observed a distinct correlation between wind speed and concentration of sea-salt larger than 10^{-11} gm up to wind speeds of 15 m/sec. He also found a linear increase in concentration of particles larger than 10^{-9} gm with increase in wave height. Results of experiments by Monahan (1968) reveal an abrupt increase in concentration of sea water droplets larger than 45 μ radius at a wind speed of approximately 9 m/sec, measured 47 cm above the sea surface.

Moore (1952) also analyzed the visibility observations at two ocean weather ships and determined that the opacity for a given humidity increases with wind speed. He attributed this increase to an observed increase in the concentration of large nuclei. Another result indicated that at lower humidities, the increase in opacity was more pronounced, and Moore believed this was due to the dehydration of larger droplets. These conclusions would indicate that the aerosol

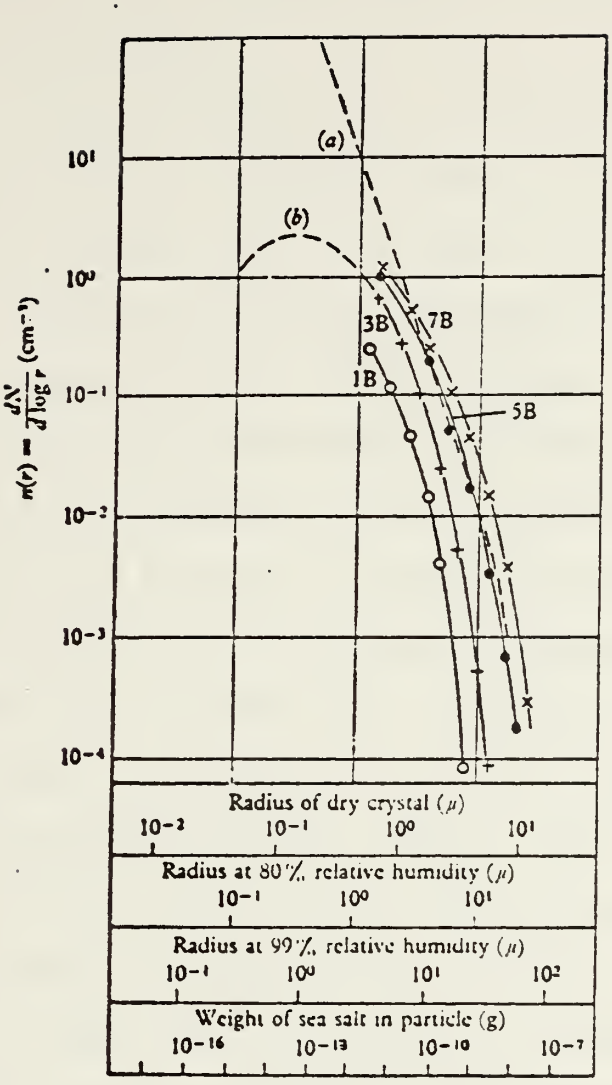

Figure 7. Size Scale and Average Size Distribution of Sea-Salt Nuclei Measured by A.H. Woodcock (Mason, 1975)

distribution is more variable and sensitive to wind speed in drier air, and this feature should be most noticeable in the larger size ranges.

As the wind speed increases over the ocean, gravity waves are generated and begin to break at a critical wind speed generally agreed upon to be near 7 m/sec. Air that is entrained by these breaking "whitecaps" rises to the surface sometime later in the form of bubbles. The principal mechanisms of sea-salt production are thought to be the direct spraying of droplets off the crests of breaking waves and the bursting of bubbles in areas of whitecaps and foam. Droplets produced by direct spraying are generally larger than 45 μ and, due to large fall velocities, are not airborne long enough to evaporate and become light enough to be transported upward (Monahan, 1968). Toba's model (1965b) showed that the net production of sea-salt particles at the sea surface seems to increase with particle mass even beyond 10^{-8} gm (20 μ), but that the transport by eddy diffusion is not sufficient to carry the particles upward against gravity beyond this size. The presence of particles larger than 10^{-8} gm in the atmosphere is generally attributed to coalescence of sea-salt droplets within and below clouds.

Some examples of residence times for different sea-salt particle sizes taken from Junge (1972) are found in Table I. It would seem then that particles in the .1 μ - 20 μ range, at least, are produced by the bursting of bubbles.

In efforts to photograph the rupture of the surface bubble film, Kientzler, et al. (1954) found that their camera

exposure was too long to capture this rapid phenomenon. However, they were able to see the formation of the "Rayleigh" jet which projects upward, continues to rise as a thin column, and then breaks into droplets of varying sizes. Day (1964) describes this process in the following manner. Each bubble, as it reaches the surface, develops a spherical film-cap which drains, thins, and bursts. Fragments of the film are thrown out and are dragged upward by the air which escapes from the bubble orifice. Water, rushing down the sides of the bubble cavity, emerges from the center as a narrow jet. A schematic of this process is shown in Figure 8. The larger drops (L) are formed by disintegration of the jet (J). Smaller particles (S) are formed by bursting of the bubble film.

Kientzler's experiment was significant in that no droplets of large enough size to be resolved by the film and optical system were observed from .2 - 1.8 mm diameter bubbles until after the jet formation. This was interpreted to indicate that the larger droplets are not produced when the bubble film is broken. On the average, the droplets produced by the jet mechanism were approximately 1/10 of the original bubble size. 1 mm diameter bubbles were observed to produce droplets of approximately 50 μ radius. The smallest observed were of 2 μ radius and deduced to have been formed by a bubble of approximately .04 mm diameter. Therefore, the jet mechanism can be considered a source of salt particles greater than 10^{-12} gm (1 μ).

	Residence Time τ, days			
	M = 10^{12} grams	M = 10^{-11} grams	M = 10^{-10} grams	M = 10^{-9} grams
Toba's value w_l for 80% relative humidity	86	17	2.9	0.32
Toba's value w_l for 91.4% relative humidity	59	11	2.1	0.23
Eriksson's estimate from sedimentation	82	16	2.6	0.4
Eriksson's estimate from production	3.5	1.0	0.6	0.5
Our estimate*	1.9	1.6	1.0	0.26

Table is taken from *Toba* [1965*a*, Table 2]. The variable M is the mass of particles.

Table I. Residence Times of Sea-Salt Particles over the Oceans

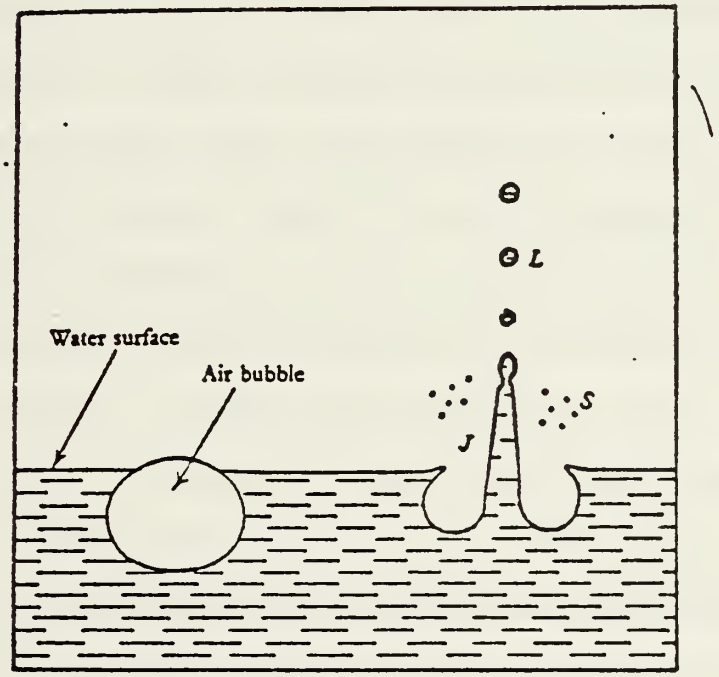

Figure 8. The Formation of Sea-Salt Droplets by the Bursting of Bubbles (Mason, 1975)

Mason (1954) utilized a cloud chamber to study bubble behavior in both distilled and salt water. After expansion, a dense cloud of tiny droplets was observed rising vertically in the space above the salt water, but not above the distilled water. Bubbles of 3 mm diameter produced 100-200 of these condensation nuclei, the majority of which are estimated to have salt contents between 10^{-15} gm and 2×10^{-14} gm. This would correspond to droplets of approximately .1 μ to .3 μ radius at 80% relative humidity. Mason also observed a second group of droplets produced by the shattering of the bubble film. These were projected sideways at an angle of ten to 15 degrees above the horizontal and slightly larger, containing between 2×10^{-12} - 5×10^{-10} gms of salt. However, the numbers of these droplets were always small, on the average, there was only about one droplet in this size range.

The number of droplets which rise vertically from a bursting bubble is strongly related to the state of compression of the film of organic material on the water surface. Paterson and Spillane (1969) have shown that with an increase of film pressure the number of nuclei produced decreases markedly. This would indicate that the production of sea-salt droplets originating from the bubble film mechanism would be suppressed in regions of high organic activity on the sea surface. Aerosol samples taken by Woodcock (1972) over Hawaiian and Alaskan seas may help explain where the transition between the jet and film sea-salt production mechanisms occurs. His observations, using an improved slide collection

technique, show an increased average particle production for sea salt particles less than 2×10^{-14} gm (.3 μ radius) in Hawaii where marine organic productivity is low. In contrast, the mean distribution curve for particles over the organically rich Gulf of Alaska fails to indicate an increased slope of the concentration curve among particles of the same size range. These curves are shown in Figure 9. The presence of surface active films arising from the biologically productive Alaskan waters is thought to suppress the production of film droplets.

Statistical analysis by Meszaros and Vissy (1974) showed that with increasing particle radius the correlation between wind speed and chloride concentration increased. This meant that smaller chloride particles are formed by the bubble film mechanism than by direct spraying. The distribution curve gives evidence that the transition between these two chloride formation mechanisms lies between .2 μ and .4 μ. Thus the maximum at .1 μ gives the maximum of chloride particles formed by the bubble film process.

Moore (1952) found evidence that the particle concentrations below 1 μ are not correlated with wind speed. This would indicate that most of the particles between .1 μ and 1 μ are not produced by bursting bubbles. Other experiments using the effects of relative humidity on particle growth indicate that a considerable proportion of marine particles between .1 μ and 1 μ must differ in composition from sea-salt (Junge, 1972). Meszaros and Vissy (1974) found that, in this size range, sodium chloride varied from 4-50% of the

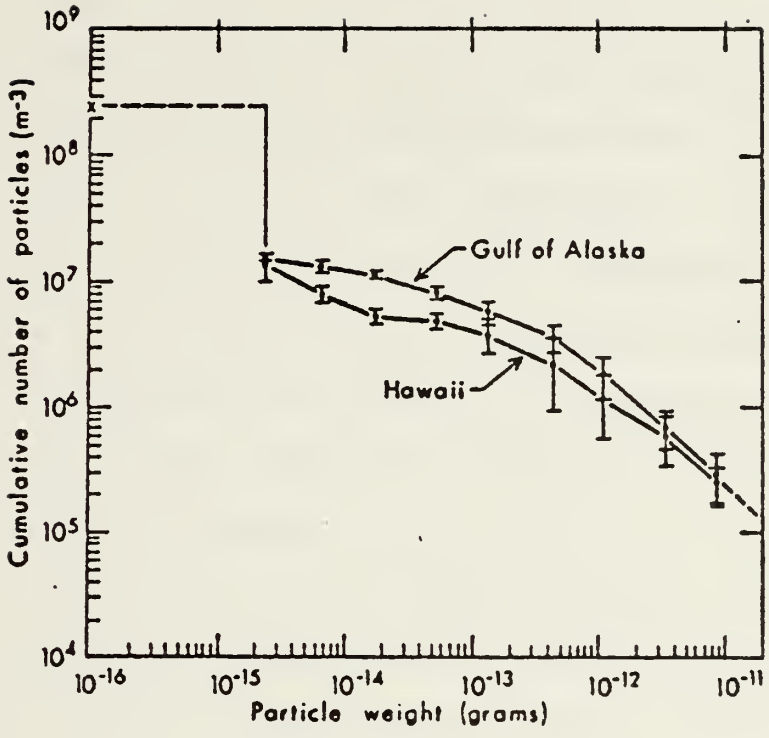

Figure 9. Distribution Curves over Alaskan and Hawaiian Waters (Woodcock, 1972)

concentration for all particles. The observations by Hidy et al. (1974) off the coast of Southern California revealed that 11% of the aerosol sampled contained sea-salt, the remainder being a combination of sulfates, nitrates and soil dust.

E. AEROSOL MODEL

Recently, various aerosol models have been developed in an attempt to accurately describe marine aerosol distributions as a function of one or more parameters. This is essential for the calculation of optical propagation through the atmosphere as aerosols scatter and absorb energy. Since the aerosol distribution is known to be dependent on relative humidity and wind speed, these two variables usually are the key parameters of each model.

One model in particular has been developed by Fitzgerald and Ruskin (1977) on the basis of the North Atlantic observations. They applied the effects of relative humidity on the equilibrium growth of aerosol particles to the sea-salt mass distribution determined by Lovett (1975) in the North Atlantic. Lovett presents empirical log radius mass distributions in the form of the following power law:

$$\frac{dN}{d \log r_d} = C\, r_d^{-\nu} \qquad (3)$$

where r_d is the dry particle radius and C and ν depend on the wind speed V in the following manner:

$$\nu = 3.317 - .03\, V \qquad (4)$$

and $$C = 0.2 - 0.0196\ V + 0.0121\ V^2 \qquad (5)$$

These expressions are valid only over a wind speed range of 3-17 m/sec^{-1}.

Formulae have been derived (Fitzgerald, 1975) for the equilibrium size of aerosol particles composed of a single pure salt as a function of relative humidity. For a sodium chloride particle the relationship between particle radius and relative humidity may be expressed as

$$r = \alpha\ r_d^{\beta} \qquad (6)$$

where α and β are functions of the relative humidity as described by Fitzgerald (1975). Equations (3) and (6) are combined to describe the aerosol size distribution as a function of relative humidity and wind speed, giving

$$\frac{dN}{d \log r} = \frac{c}{\beta} (\alpha^{\nu/\beta}) (r^{-\nu/\beta}) . \qquad (7)$$

Comparison between the aerosol distributions derived from the above model and those observed in two coastal marine environments is made within this study.

III. TURBULENCE THEORY

A. BOUNDARY LAYER CONSIDERATIONS

The importance of turbulent exchange processes in the surface boundary layer has long been recognized. Panofsky (1969) describes atmospheric turbulence as consisting of horizontal and vertical eddies by which the air is mixed. The two mechanisms by which eddies are formed in the atmosphere are heating from below and wind shear. Heating produces convection and the change in wind speed with height produces mechanical turbulence. Because there is no wind at ground level, and there is usually some wind above the ground, mechanical turbulence is common. This type of turbulence increases with increasing wind speed (at a given height) and is greater over rough terrain than over smooth terrain. The terrain roughness is usually characterized by a roughness length, Z_o , which is proportional to the size of the eddies that can exist. The relative importance of heat convection and mechanical turbulence is characterized by the Richardson number, R_i . The Richardson number is a measure of the relative rate of conversion of convective to mechanical energy. For example, negative Richardson numbers of large magnitude indicate that convection predominates resulting in strong vertical motion. As the mechanical turbulence increases, the Richardson number approaches zero.

Finally, as the Richardson number becomes positive, the thermal stratification becomes stable and damps the mechanical turbulence. For $R_i > 0.25$, vertical mixing disappears.

The effect of the wind on the underlying surface is termed the shearing or Reynolds stress, τ , and is characterized by a downward momentum transfer. The Reynolds stress may be represented by

$$\tau = -\rho \langle u'w' \rangle \qquad (8)$$

where u' = fluctuating horizontal wind velocity

w' = fluctuating vertical wind velocity

ρ = density of air

It is convenient to express Reynolds stress in terms of the friction velocity U_* so that

$$\tau = \rho U_*^2 \qquad (9)$$

where U_* is constant throughout a region of constant momentum flux. Hence, U_* is a measure of the downward transfer of momentum in the lower 50 meters of the atmosphere. Over the ocean an increase in the near surface winds would lead to a greater momentum and energy transfer for surface wave and sea-salt aerosol production. The relationship between the turbulent transfer of heat and moisture in the marine boundary layer and the generation and transfer of aerosols is not well known and, unfortunately, is not investigated in this study.

B. MOMENTUM TRANSFER, U_*, RELATIONS

A thorough discussion of the boundary layer expressions is presented in several references, e.g. Lumley and Panofsky (1964). The similarity approach of Monin and Obukhov (1954) is used to define a representative length scale, L , for the surface layer of the atmosphere,

$$L = \frac{-U_*^3 \, T_o}{kg \, \overline{w'T'}} \qquad (10)$$

where g = gravitational acceleration

T = ambient temperature

k = von Karman constant = 0.35

The selection of the Monin-Obukhov length as a stability scaling parameter is based on the assumption that friction velocity, U_* , and vertical heat flux ($\overline{w'T'}$) are constant in the surface layer. This scaling length, using dimensional analysis, leads to the development of a dimensionless function, $\phi_m(Z/L)$, which can be used to represent the mean horizontal wind variation with height, $d\bar{u}/dZ$, in the surface layer. The following expression is the empirical relationship for the wind shear in this development,

$$\frac{d\bar{u}}{dZ} = \frac{U_*}{kZ} \, \phi_m(Z/L) \qquad (11)$$

As vertical turbulent heat flux ($\overline{w'T'}$) decreases to zero, indicating neutral stability, $\phi_m(Z/L)$ must approach 1 if Equation (11) is to take on its expected form under neutral conditions. Assuming that convective mixing is negligible

under neutral conditions it follows that for values of ϕ_m (Z/L) near 1 or Z << 1 mechanical turbulence is of primary importance. Thus, the absolute magnitude of L becomes an indicator of the vertical extent to which mechanical turbulence controls the turbulent regime.

Observational experiments by Businger et al. (1971) produced a definite relationship between the Richardson number, R_i ,

$$R_i = \frac{g(\partial\theta_v/\partial Z)}{\bar{\theta}(\partial u/\partial Z)^2} \tag{12}$$

and the Monin-Obukhov length, L , where θ_v is the virtual temperature. The following expressions are approximations for the unstable and stable conditions respectively,

$$Z/L = R_i \tag{13}$$

$$Z/L = \frac{R_i}{1-\alpha R_i} \tag{14}$$

where α is an empirically derived constant equal to 0.5.

Of interest in this study is the rate of viscous molecular turbulent kinetic energy dissipation, ε . Wyngaard, et al. (1971) considered the dependence of ε on momentum fluxes and height in deriving the following empirical expression

$$\varepsilon = U_*^3/kZ\ \phi_\varepsilon\ (Z/L) \tag{15}$$

Since Z/L and R_i are functionally related, equations (11) and (15) can be rewritten as

$$\frac{d\bar{u}}{dZ} = \frac{U_*}{kZ}\ f_m\ (R_i) \tag{16}$$

and $$\varepsilon = U_*^3/kZ\ f_\varepsilon\ (R_i) \qquad (17)$$

where f_m and f_ε are stability corrections equal to 1 under neutral conditions. In near neutral conditions, the turbulent kinetic energy production is assumed to be equal to the rate of molecular dissipation of turbulent kinetic energy and from equations (16) and (17) the following relation is valid

$$\varepsilon = U_*^2(\partial\bar{u}/\partial Z) \qquad (18)$$

Assuming neutral conditions, the combinations of equations (16) and (18) yields

$$U_* = (\varepsilon kZ)^{1/3} \qquad (19)$$

Now the friction velocity U_* can be estimated from either mean wind profiles using the integrated form of equation (16) or from velocity fluctuation data involving turbulent energy dissipation by using equation (19). The latter approach is used in this study.

IV. DATA COLLECTION

A. DURATION AND LOCATION

Aerosol and meteorological data for this study were made available through Calspan Corporation, Buffalo, New York, from two separate experiments. During a ten day period in February 1977, Calspan Corporation provided limited meteorological and cloud physics support during a study of marine boundary layer phenomena conducted on the Gulf of Mexico (Mack and Katz, 1977). The experiment was performed on the Naval Coastal Systems Laboratory's (NCSL) offshore platform "Stage I" located approximately 20 km SW of Panama City, Florida as depicted in Figure 10.

A second experiment which provided data for this study was conducted along the coastal waters of Southern California (Figure 11) during a 12 day period in July 1977 aboard the Naval Postgraduate School (NPS) R/V Acania. Under contract from NPS, Calspan Corporation provided limited meteorological and aerosol physics support during a study of air quality parameters and marine boundary layer characteristics (Mack, 1977). This region contains primary shipping lanes and a number of drilling platforms all of which contribute to atmospheric contamination.

The following discussion will be limited to equipment used to measure the meteorological parameters actually analyzed in this study. A listing of the Panama City and

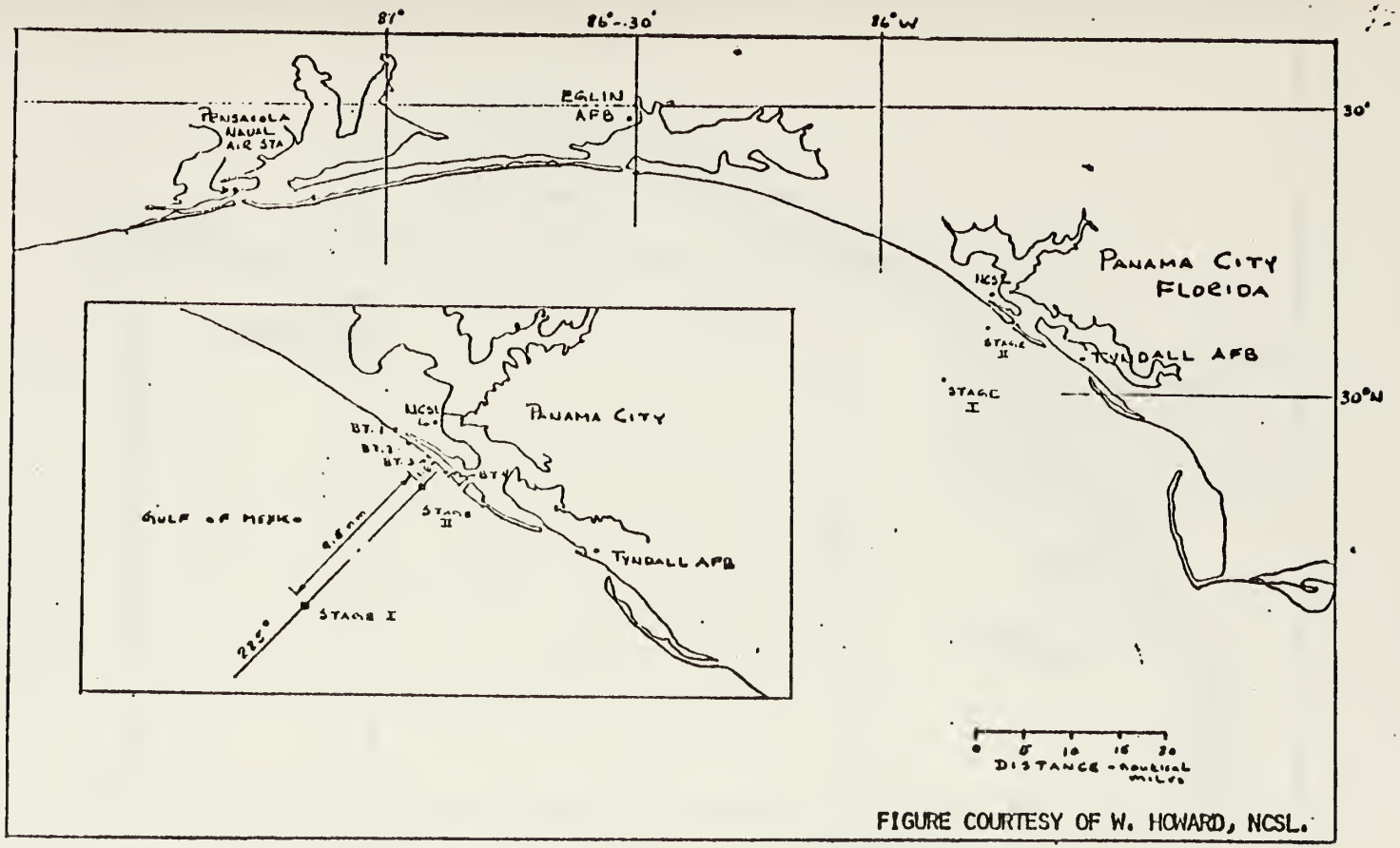

Figure 10. Location of NCSL Offshore Platform "Stage I"

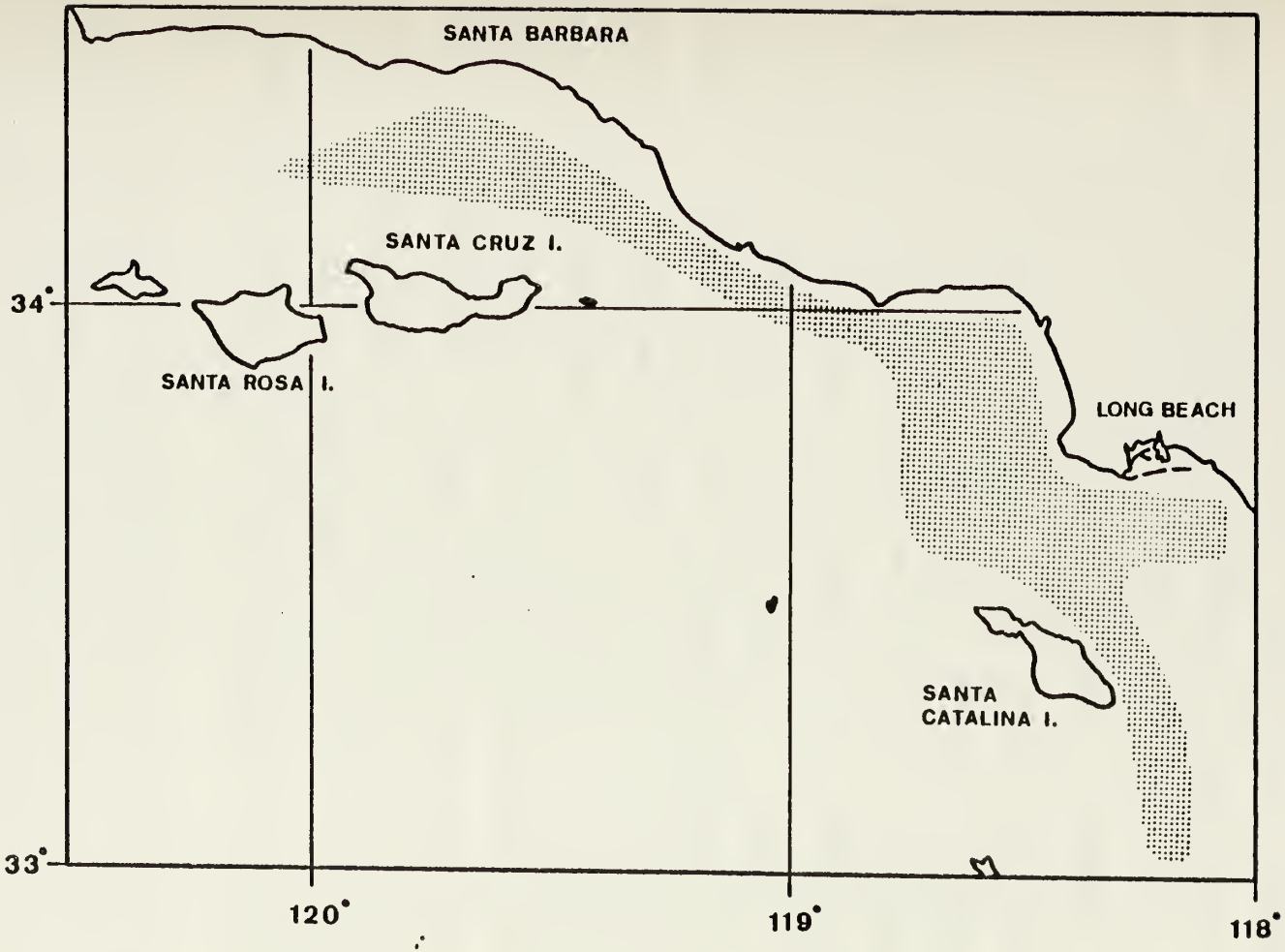

Figure 11. Location of Southern California Cruise

Southern California data may be found in Tables V and VI, respectively, at the end of the text.

B. PANAMA CITY INSTRUMENTATION

"Stage I" provided a stable platform for measuring the meteorological parameters necessary to describe and study the aerosol distribution and behavior in the marine boundary layer. The instrumentation installed by Calspan included a Sling Psychrometer, Bechman-Whitley wind system, Gardner small particle detector, and Royco Model 225 Particle Counter. The wind speed and direction was monitored continuously at the 20 meter level while wet and dry bulb temperatures were obtained hourly at the 17 meter level. A Foxboro temperature system (4 sensors) provided continuous temperature measurements at 4 levels; sea surface, 4.5, 9.0 and 24.5 meters. This data was recorded in an hourly log. Ten minute averaged aerosol size spectra were obtained continuously with the Royce counter at the 17 meter level, and a printout of aerosol concentration in 5 size intervals was provided every ten minutes. The Gardner Counter measured the concentration of particles greater than .0025 μ diameter on an hourly basis.

The majority of the time the Royco instrument operated in "threshold" mode where number concentration (per 2.8 liters) of particles greater than the following size ranges were measured: 0.5 μm, 0.7 μm, 1.4 μm, 3.0 μm, and 5.0 μm diameter. For a shorter period of time the instrument was operated in the "window" mode producing number concentrations between the

above size ranges. The particle counter and sensor are shown in Figure 12. The environmental air was drawn continuously through a sampling line of 3 meter length and 5 cm inside diameter. The flow rate through the counter's sensing volume was set at 2.8 liters per minute.

The Royco Model 225 sampler utilizes a near forward scattering optical system (Figure 13) which is ideal for monitoring large volumes of ambient gases where suspended particles can vary widely in composition, size, and optical properties. The aerosol is drawn through the sensor into a beam of focused light. As each particle passes through the illuminated volume, it scatters a pulse of light which is then detected by a photomultiplier tube. The photomultiplier output is then processed elctronically to produce a pulse height spectrum from which the particle size spectrum is deduced. The height of each pulse is proportional to the square of the diameter of the particle.

Whitby and Liu (1973) note that the important characteristics of an optical counter are the sampling flow rate and the size of the optical viewing volume. The sampling flow rate determines the minimum counting period needed to obtain a statistically accurate count, and the size of the optical viewing volume determines the maximum aerosol concentration the instrument can accept without loss of particle count due to "coincidence", i.e., the loss of particle count due to the presence of more than one particle in the optical viewing volume at the same time. The viewing volume of the Royco 225 is 4.0 mm^3 and the collection aperture half angle is 25 degrees.

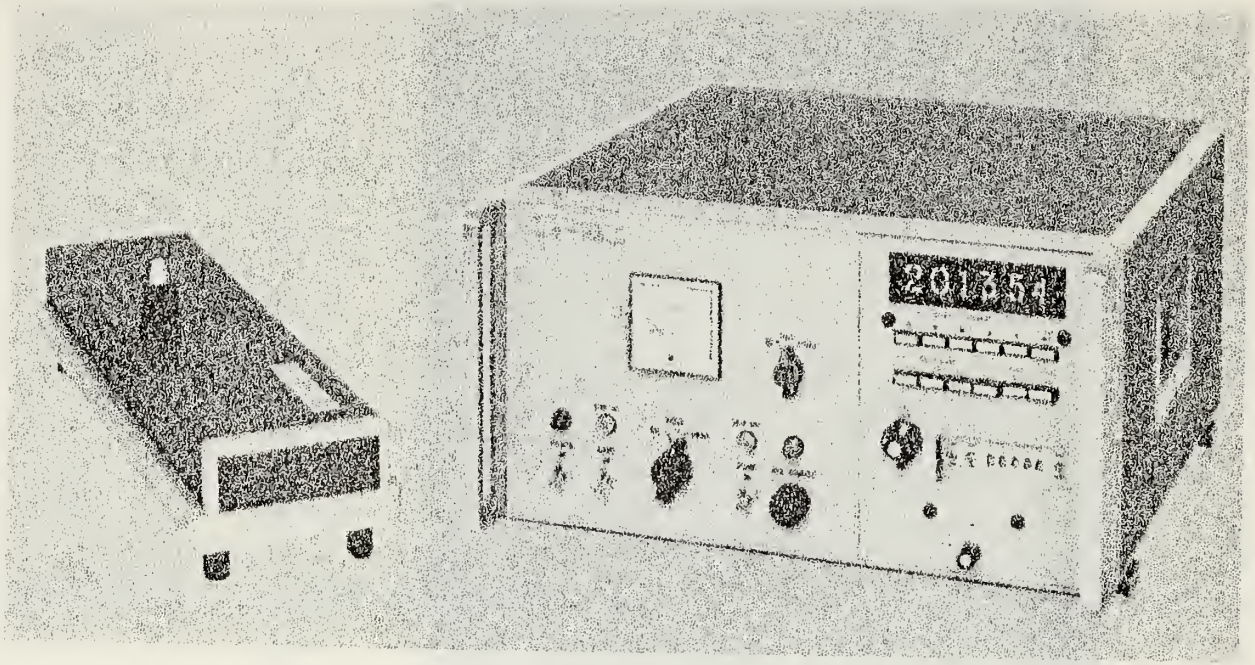

Figure 12. Royco 225 Particle Counter and Sensor

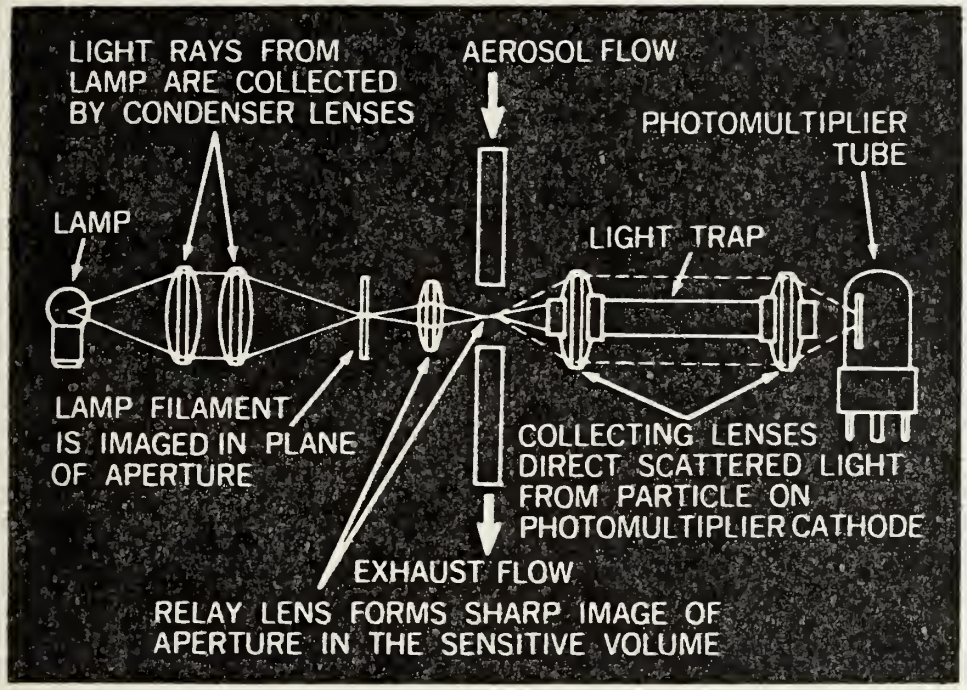

Figure 13. Near Forward Scattering Optical System

This model is also equipped with a sheath air inlet which diverts part of the aerosol stream through an external filter before reentry to the viewing volume. This sheath improves the performance of the instrument by preventing the recirculation of particles in the optical chamber and by confining the aerosol stream to a narrower region. Thus, the broadening of the pulse spectrum due to variation in illuminating intensity is reduced.

C. SOUTHERN CALIFORNIA INSTRUMENTATION

The location of the sensors aboard the R/V Acania are shown in Figure 14. Again, a Royco Model 225 Optical Particle Counter was used to measure the aerosol concentration of the coastal marine boundary layer. This instrument was operated continuously in the threshold mode where number concentration (per .28 liters) of aerosols greater than the following size ranges were measured: 0.3 μm, 0.6 μm, 1.2 μm, 3.0 μm, and 5.0 μm diameter. The mainframe and sensor were located near the bridge of the Acania with the origin of the sampling line positioned forward of the pilot house roof at a height of 7 meters above the sea surface. The sampling line was 6 meters long with an inside diameter of 5 cm. The air was sampled through the viewing volume at a rate of .28 liters per minute. A Gardner small particle detector was again used to measure the Aitken nuclei concentration.

A sling psychrometer was used to measure the wet/dry bulb temperatures and relative humidity determined from psychometric tables for a height of 5 meters. The mean wind

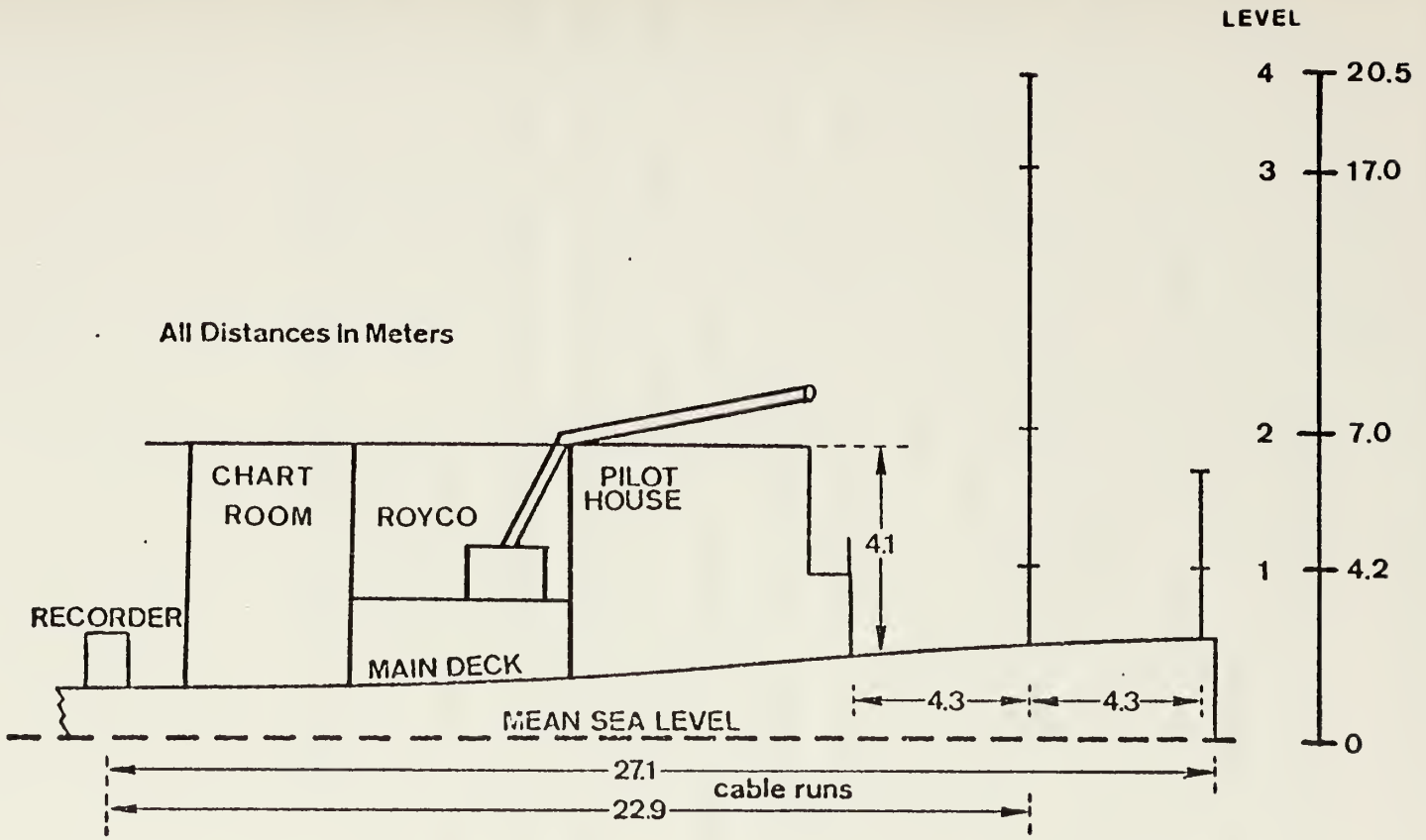

Figure 14. Sensor Locations on Board the R/V Acania

measurements were obtained at four levels using cup anemometer wind profile register systems supplied by the NPS. Calspan recorded the wind, humidity, and aerosol measurements in an hourly log.

Velocity fluctuation measurements were obtained with Thermo-Systems Model 1210 hot wire anemometer probes mounted with hot film sensors (platinum coated, 60 mil quartz fibers) installed by the NPS. The anemometer was a Thermo-Systems Model 1054B. The sensors were small enough to resolve the viscous dissipation scale without making corrections for wire length. Wind fluctuation data were recorded on a 14 channel tape recorder. The placement of these sensors required exceptionally long cable runs. Therefore, adjustments were made in the bridges for resistance and capacitance of the wirelength to insure a correct response.

The mean and fluctuation wind data were logged by the NPS developed MIDAS (Microprogrammable Integrated Data Acquisition System). This system is fully automated to sample the tailored list of sensors every 30 seconds and 20 minute averaged output values were printed.

V. ANALYSES PROCEDURES

A. VELOCITY FLUCTUATION ANALYSIS

The dissipation of turbulent kinetic energy, ε , can be related to the mean wind velocity at any given level, $\bar{u}$, and the RMS value of the velocity fluctuation, $\overline{u'^2}$, in a frequency band specified by a lower frequency limit, f_ℓ , and an upper frequency limit, f_u (Fairall, et al., 1977). The relationship is

$$\varepsilon = \frac{(4/3)^{3/2} \, (u'_{RMS})^3}{(\bar{u}/2\pi)[f_\ell^{-2/3} - f_u^{-2/3}]^{3/2}} \qquad (20)$$

In this procedure recordings were made of both the cup anemometer wind speed and the corresponding hot wire voltage output. The sensor wind speed is given by

$$v = V_o^2 + B(\bar{u})^{\frac{1}{2}} \qquad (21)$$

where v is the hot wire voltage output, and V_o^2 and B are constants obtained by laboratory calibration using a TSI Model 1125 Calibrator. Differentiation of equation (21) produces the following relationship between the velocity fluctuation and the voltage fluctuation:

$$u'_{RMS} = \frac{4v(\bar{u})^{\frac{1}{2}}}{B} \, v'_{RMS} \qquad (22)$$

Substitution into equation (20) yields

$$\varepsilon = \frac{(4/3)^{3/2}[4\nu(\bar{u})^{1/2})/B]^3 \ (v'_{RMS})^3}{(\bar{u}/2\pi)[f_\ell^{-2/3} - f_u^{-2/3}]^{3/2}} \qquad (23)$$

Values of $f_\ell = 5$ Hz and $f_u = 200$ Hz were selected for the cruise and since amplifiers with known gains, G, were required, further reduction leads to

$$\varepsilon = (3.53\times10^3)[V_o^2 + B(\bar{u})^{1/2}]^{3/2}(\bar{u})^{1/2}[v'_{RMS}/BG]^3 \qquad (24)$$

The friction velocity, U_*, was then calculated from equation (19) for each of three levels and averaged to produce over 400 values from 19-27 July. Voltage fluctuation data from level 3 proved to be erroneous and were not included in the calculations. Obviously erroneous values of U_* owing to erratic behavior were also neglected. U_* values were then averaged about the aerosol observation times to correspond to a given aerosol distribution.

B. AEROSOL ANALYSIS

Analyses were performed on 215 aerosol samples during the SC cruise which were confined to the time period of the valid velocity fluctuation measurements. The observations included date and time, humidity, relative wind speed and direction, ship's speed and heading, Aitken concentration, and aerosol concentration as determined by the Royco 225 optical counter (Table VI). Wind and ship's speeds were recorded in knots.

The analyzed aerosol observations for the PC experiment were limited to 137 cases during the period 18-23 February. Cold frontal passage at approximately 0000Z, 24 February and subsequent advection of continental dust through 25 February were reasons for neglecting the aerosol samples for these days. Aerosol counts prior to 18 February were determined with the Royco instrument in the window mode and were not included in this study. Observations were generally made hourly and recorded in a log. They included date and time, humidity, wind speed and direction (knots), Aitken concentration, and data from the optical particle counter (Table V).

Computer programs were developed to plot the aerosol size distribution as a function of radius (R) in microns versus $dN/d \log R$ (cm^{-3}) where N is the number of particles greater than a given radius as measured by the Royco instrument. The program also included provisions to plot size distributions predicted by Fitzgerald's model. For this the observed relative humidity and wind speeds were used with equation (7). Initially the average aerosol distributions for both the SC and PC experiments were computed and compared to the respective predicted model distributions.

Subsequently, the variations in the average aerosol distributions with respect to four different categories of wind speed, relative humidity, and friction velocity were plotted for the SC data. The categories chosen for each of the above respective parameters are as follows: 0-2, 2-5, 5-8, 8-12 m/sec; 90-99, 80-90, 70-80, and 60-70 percent; and 0-.15, .15-.25, .25-.35, .35-.70 m/sec.

Friction velocity data was not available from the PC experiment; therefore, variations in the aerosol distributions were plotted with respect to categories of wind speed and humidity only. Because of essentially different meteorological conditions, the categories were chosen as follows: 0-3, 3-7, 7-10, and 10-15 m/sec; and 85-99, 70-85, 55-70 and 40-55 percent.

Visual inspection of these plots may indicate satisfactory relationships between the aerosol concentration and the above parameters. However, a statistical means of viewing these relationships was also deemed necessary. Wind speed, humidity, and U_* values were cross correlated with number concentration of particles in graduated size ranges. This procedure was accomplished by a Biomed Regression/Correlation computer program which produced corresponding correlation coefficients.

The nature of the diurnal variation of the aerosol concentration during the SC and PC experiments was investigated in this study. A computer program averaged the aerosol concentrations, wind speeds, humidities, and friction velocities about each hour and plots showing variations with time are produced. The aerosol plots depict the number of particles per cm^3 within specified size ranges versus time. The SC data produced curves representing the number of particles between the following size ranges: .15-.30 μ, .30-.60 μ, .60-1.5 μ, and 1.5-2.5 μ radius. Diurnal variation of concentration for the PC data utilized the following slightly different size ranges: .25-.35 μ, .35-.70 μ, .70-1.5 μ, and 1.5-2.5 μ radius.

Finally, diurnal variations of the aerosol size distribution for the SC and PC experiments were calculated using techniques similar to those described above. Average size distributions for the following two time periods were plotted: 0000-1200 hrs and 1200-2400 hrs.

C. ERROR ANALYSIS

The optical particle counter has an advantage over the membrane filter or impactor sampling techniques. For example, the latter require the samples to be taken to a lab for microscopic inspections and the aerosols may possibly be disturbed or altered due to contamination. Although the optical counter provides continuous "in situ" aerosol measurements, there are ample causes for counting errors. Because light scattering is a function of size, shape, and refractive index of the particles, careful calibration is necessary.

The Royco 225 model counter used in these experiments was calibrated using monodisperse latex spheres of known refractive index (1.6). Laboratory experiments by Lieberman and Allen (1969) showed a good correlation between the theoretical response curve for a near forward optical system and measurements using latex sphere and glass beads of refractive index 1.6 (Figure 15). Of most significance is the "fold" in the curve or zone of multi-valued response in the region of 1 μ diameter. Figure 16 is provided to illustrate how the response curve varies with particles of different refractive index. It is evident that when measuring particles of refractive index 1.6, a zone of ambiguity exists between

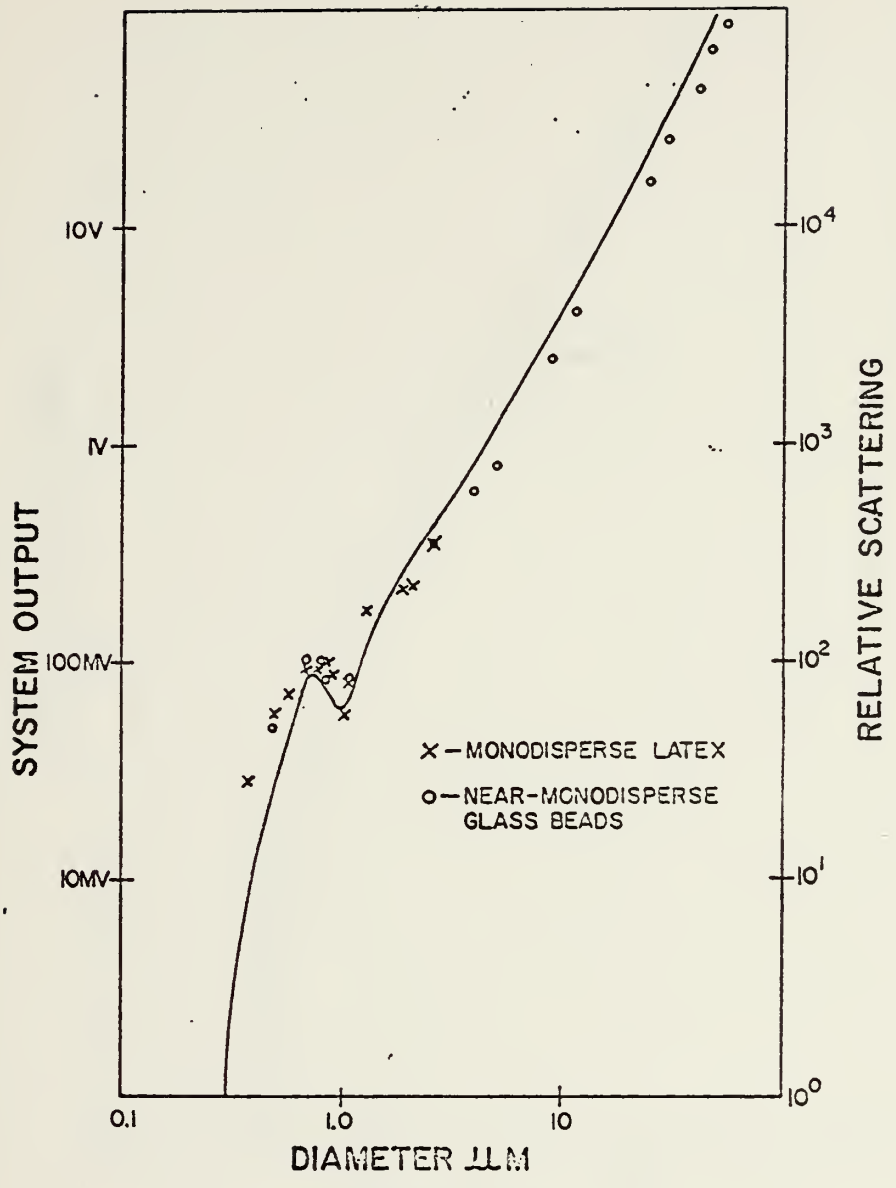

Figure 15. Theoretical Response Curve and Experimental Results for a Forward Scattering System

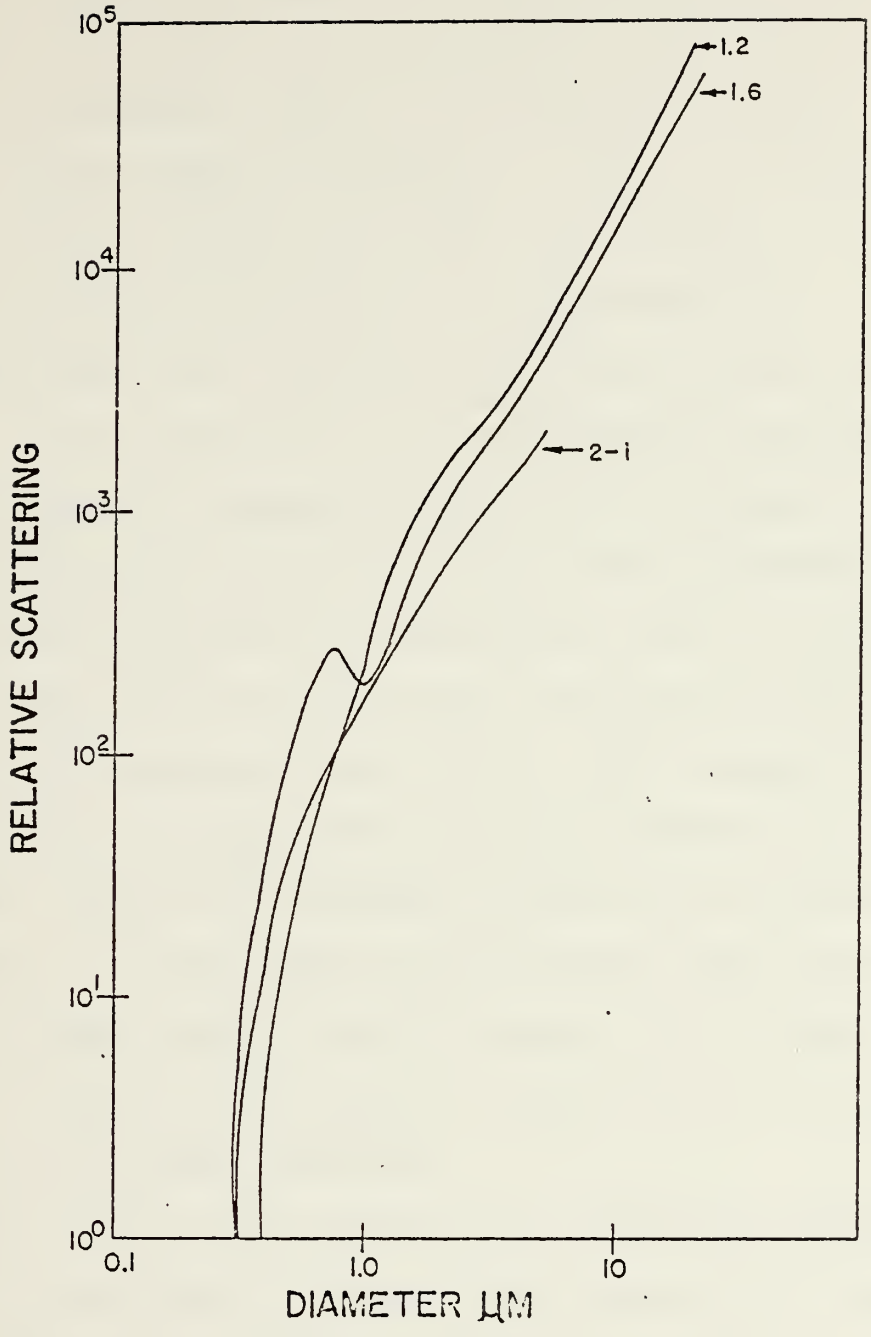

Figure 16. Dependency of the Response of a Forward Scattering System on Refractive Index

approximately .3 μ and .6 μ radius and may vary with the aerosol refractive index. Lieberman and Allen (1969) state that the instrument will still produce valid data if the zone is encompassed within a size range or channel. Since the SC counter measured between .3 μ and .6 μ radius and the PC counter between .35 μ and .70 μ radius, it is assumed that this multi-valued zone is compensated for.

Counting errors can also arise from flow rate considerations. If the particle sizes are large and the number of particles small, enough particles must be counted to obtain good statistical resolution. When a small random number of particles is counted, the statistical error in counting is equal to the ratio of 1 over the square root of the number of particles counted (Zinky, 1962). The counter should be operated over a longer time period (10 minutes) to sample a larger volume or an increase in the flow rate will reduce the error. It then seems quite possible that the flow rate of the counter used in the SC cruise (.28 liter/min) provided too small of a sampling volume to obtain an accurate count of the larger particles.

Zinky (1962) also states that a vertically aligned inlet tube is recommended to prevent any deposition in the line due to settling. It has already been mentioned that the sampling lines used in each experiment were considerably long and aligned horizontally. Many of the larger particles may not have remained airborne long enough to reach the illuminated volume.

Errors in the calculation of the friction velocity may have come from various sources. Since calculation of U_* from Equation (19) is only valid for near-neutral conditions, any substantial departure of the Richardson number from zero would result in inaccurate values. The measurement of the dissipation of turbulent kinetic energy was large dependent on the accuracy of the voltage output. The signal response is sensitive to electromagnetic energy, and any local radio or radar transmission may introduce noise to the system. Additionally, under the light wind conditions which prevailed on the SC experiment, the lateral motion of the anemometers due to ship pitch and roll may have resulted in erroneously high readings.

VI. RESULTS

The data from the Southern California (SC) cruise proved to represent an atmosphere somewhat different from a typical marine environment. The Aitken particle population averaged almost 8500 cm^{-3} which is about 4 times higher than that observed by Hidy, et al. 130 km west southwest of Los Angeles. This high concentration is suspected to be due to a combination of pollution from merchant ships' exhaust, combustion from the drilling platforms, and offshore flow from the nearby populated coastal cities.

The average wind speed and relative humidity were 3 m/sec and 86 percent, respectively. This data was used to compute the prediction from Fitzgerald's model (Eq. 7) which is compared to the average SC distribution in Figure 17. The vertical bars represent one standard deviation either side of the mean. There is generally good agreement between the two below .4 μ radius, with a larger experimentally observed concentration above this range. Although sea-salt production should have been minimal during this time period because of low wind speeds, the characteristic hump at around 1 μ, to a certain extent, reflects the contribution by sea salt nuclei. A similarity exists here with Moore and Mason's (1954) observation of a discontinuity where the slope changes and becomes rather steep in the region of the larger size range. The larger concentration in this range may be solely

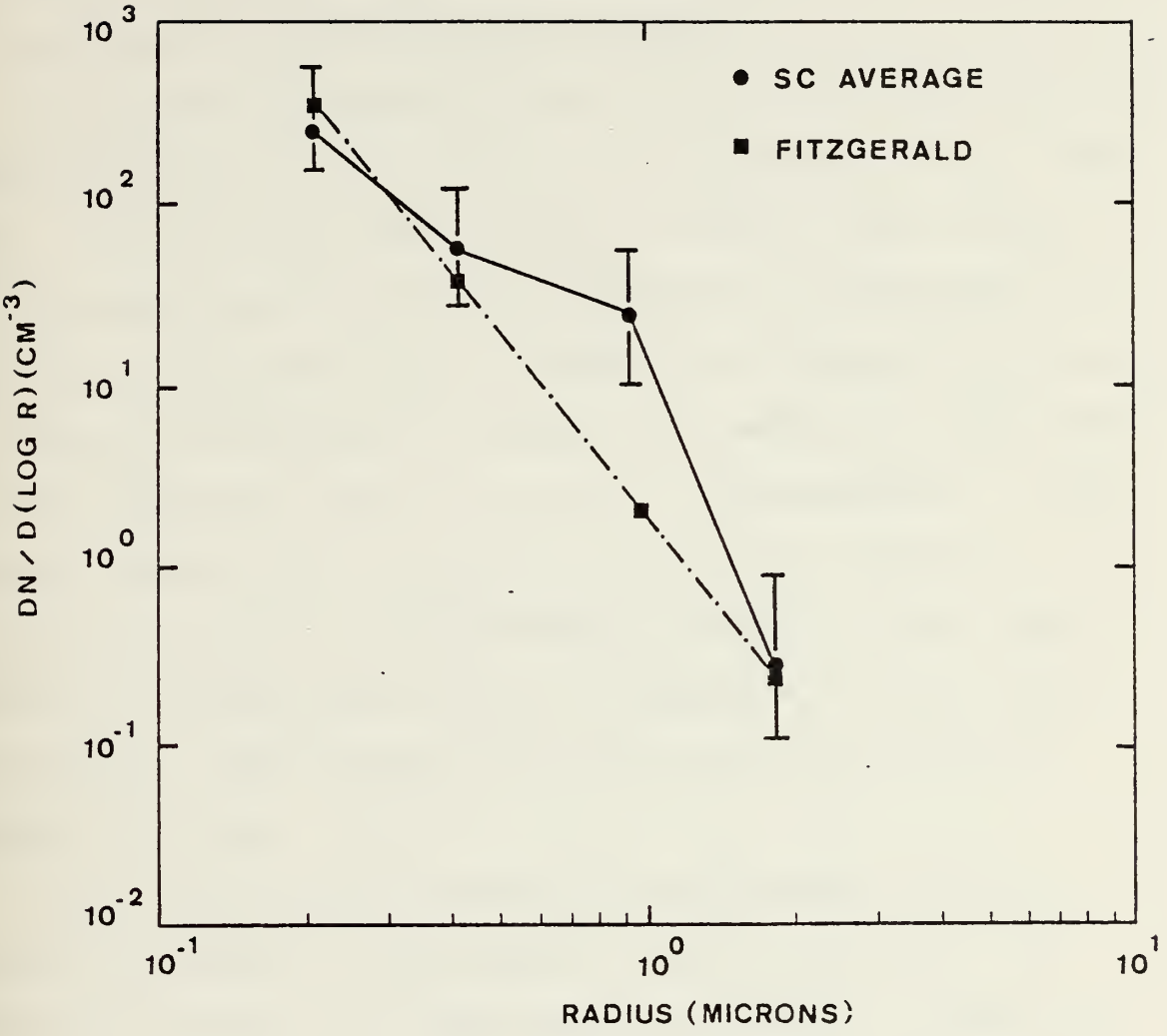

Figure 17. Average Aerosol Size Distribution for the SC Experiment and Distribution Predicted by Fitzgerald's Model

due to the influence of atmospheric contaminants such as combustion by-products, soil dust, or smoke. Considering previous experiments, this range does indeed contain a mixture of both continental and marine aerosols possibly resulting in the increase over Fitzgerald's model.

As previously mentioned, the low flow rate of the optical counter may account for the low concentrations at 2 μ. However, since the wind speed reached 8 m sec^{-1} only 6 times, this may have been a truly representative concentration of droplets as agreement is also shown with Fitzgerald's curve.

Figure 18 presents the synoptic situation for three days at the beginning, middle, and end of the experiment. A persistent thermal low is located in the desert area of Southern California and the isobaric pattern off the coast reflects a rather weak gradient. Therefore, smaller scale circulations should prevail in this area of little or no synoptic forcing.

Plots showing the variations of the average distributions with respect to wind speed, relative humidity, and friction velocity (U_*), are shown separately in Figures 19, 20, 21. The number of observations in each category is placed in parentheses. These figures indicate that the size distribution has a better relationship with the relative humidity than to the wind speed and U_* . Correlation coefficients between these parameters and the number concentration of particles in a given size interval are produced in Table II. Since diurnal variations tend to reflect a negative relationship between relative humidity and wind

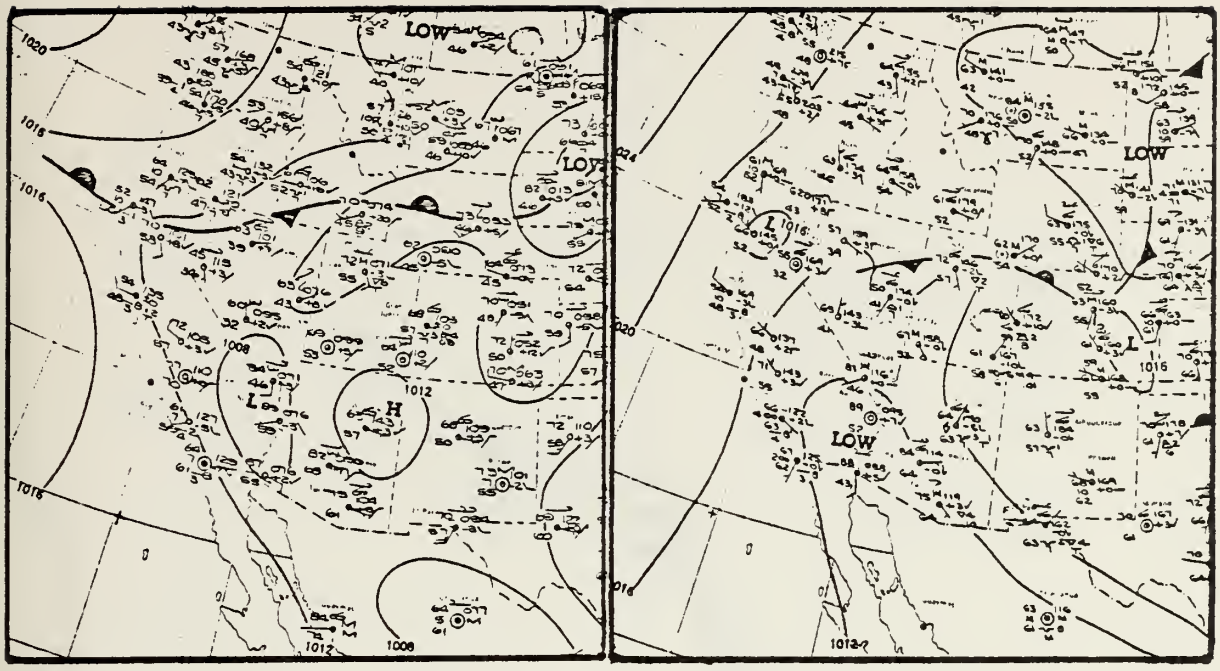

19 JUL

23 JUL

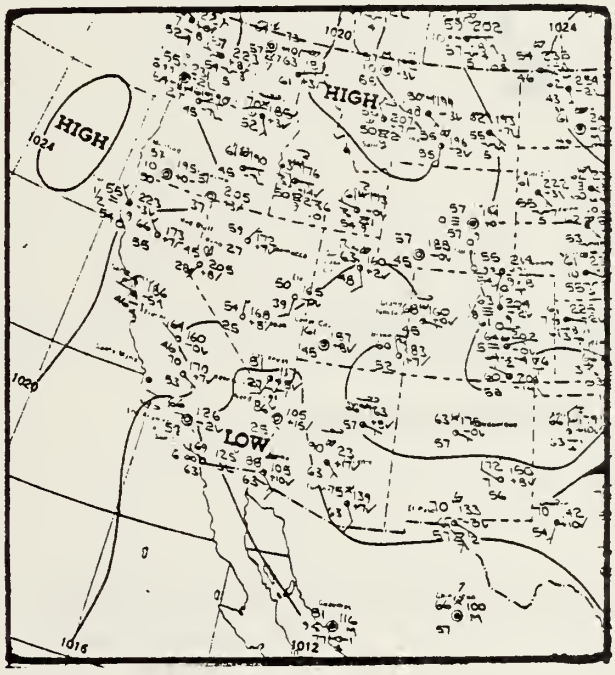

26 JUL

Figure 18. Synoptic Situation during the SC Experiment

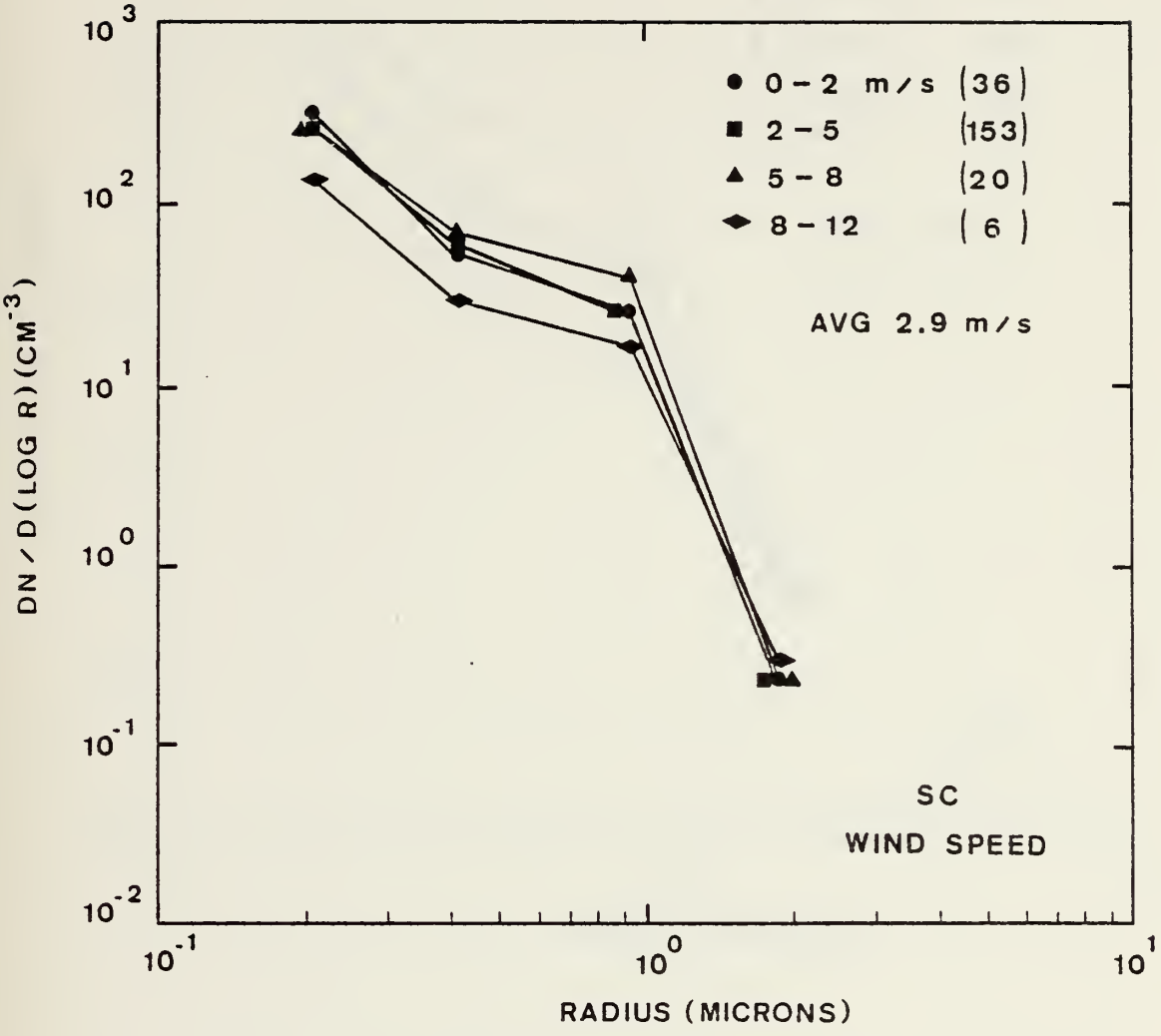

Figure 19. Variation of SC Size Distribution with Wind Speed

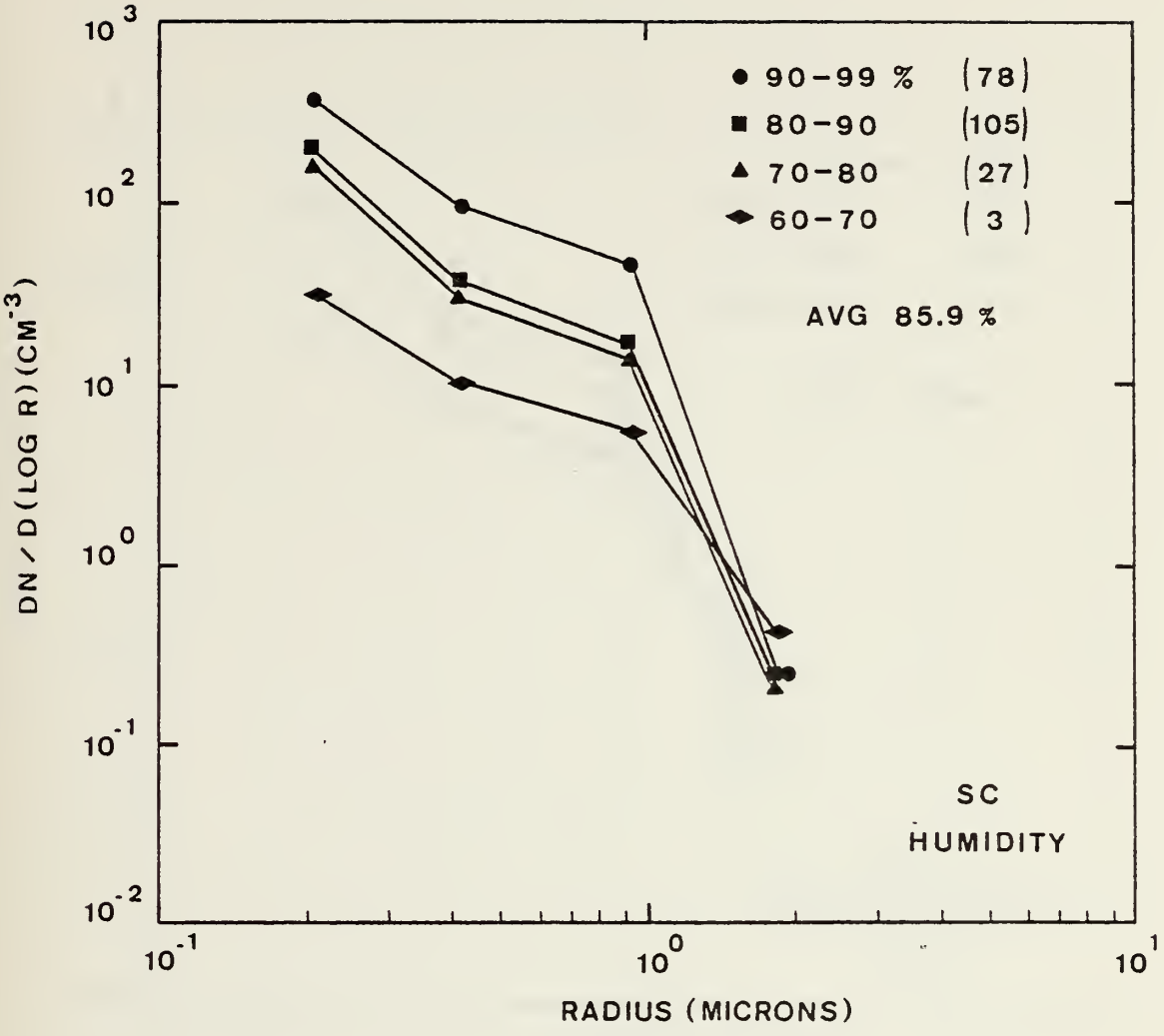

Figure 20. Variation of SC Size Distribution with Relative Humidity

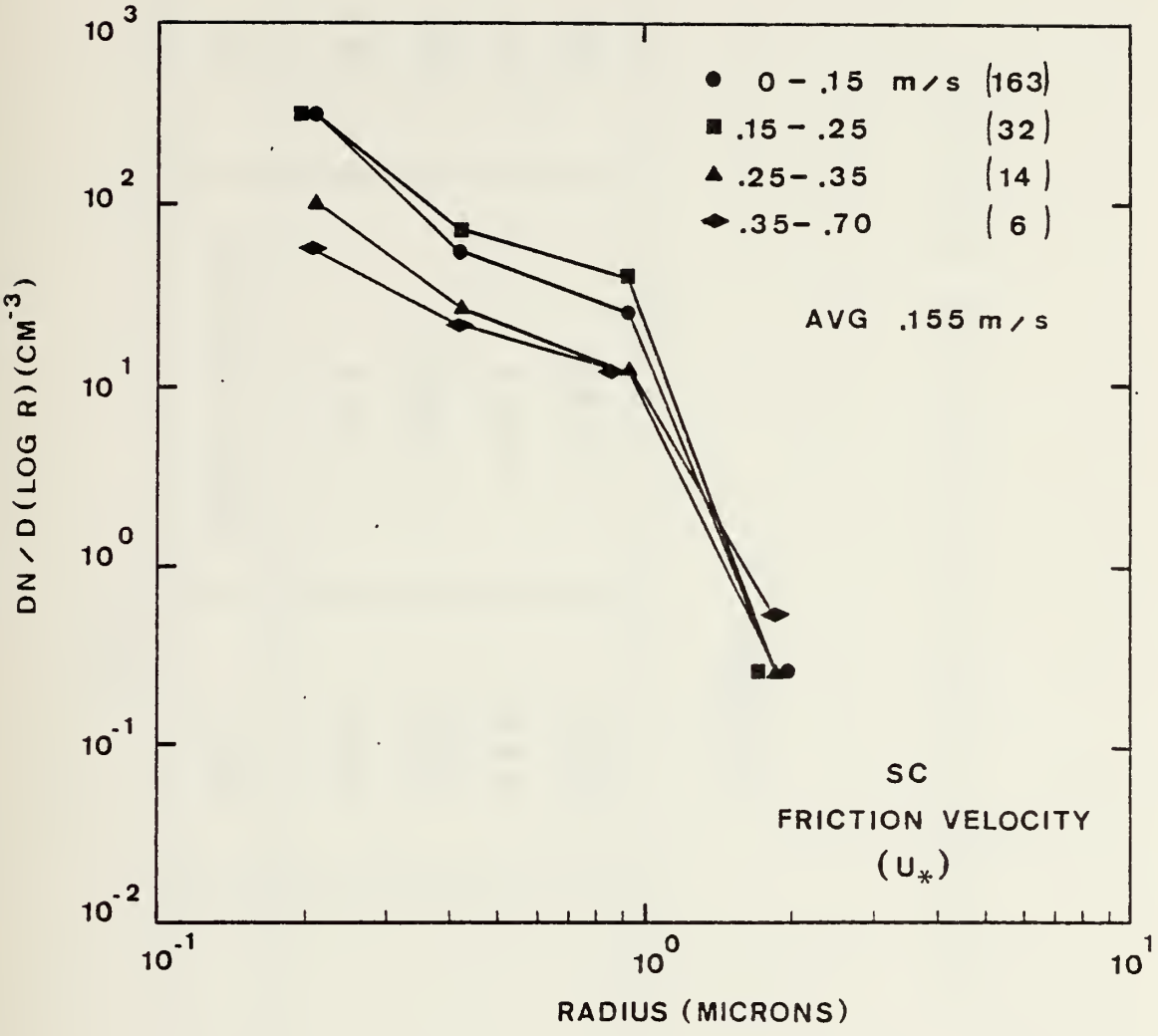

Figure 21. Variation of SC Size Distribution with Friction Velocity

SC

INTERVAL	RH	WIND SPEED	U_*
.15 – .30 μ	.375	–.127	–.162
.30 – .60 μ	.383	–.056	–.107
.60 – 1.5 μ	.376	–.017	–.077
1.5 – 2.5 μ	–.037	–.022	.132

TOTAL

Table II. Correlation Coefficients for the SC Experiment

speed, the results in this table are not surprising. The negative correlation of relative humidity with the concentrations in the large size range indicates that sedimentation of large droplets, which grow with increasing humidity, is most important when the wind speed and sea surface production of salt nuclei are weak. Although these larger droplets also exhibit a small positive correlation with U_* while the wind speed correlation remains negative, this result does not appear to be significant.

An attempt was made to examine the influence of stability on the size distribution. The summer months are characterized by the occurrence of stratus and fog off-shore below the marine inversion. Two days are compared with the assumption that they represent the unstable and stable atmospheres. According to the daily observation log, stratus clouds in the morning becoming stratocumulus by afternoon were observed on 19 July. 26 July was characterized by clear skies. The average distribution for both days is presented in Figure 22. The correlation coefficients between concentration and wind speed and U_* show a trend toward positive values from the stable to the unstable day with U_* eventually becoming positively correlated in the unstable day (Table III). The increase in the size distribution on 26 July in the size range greater than .3 μ seems to be due to increase in the average wind speed and occasional gustiness as whitecaps were reported during the afternoon. The stable stratification assumed in this case allows generated sea-salt nuclei to accumulate and the concentration to increase at the 7 meter

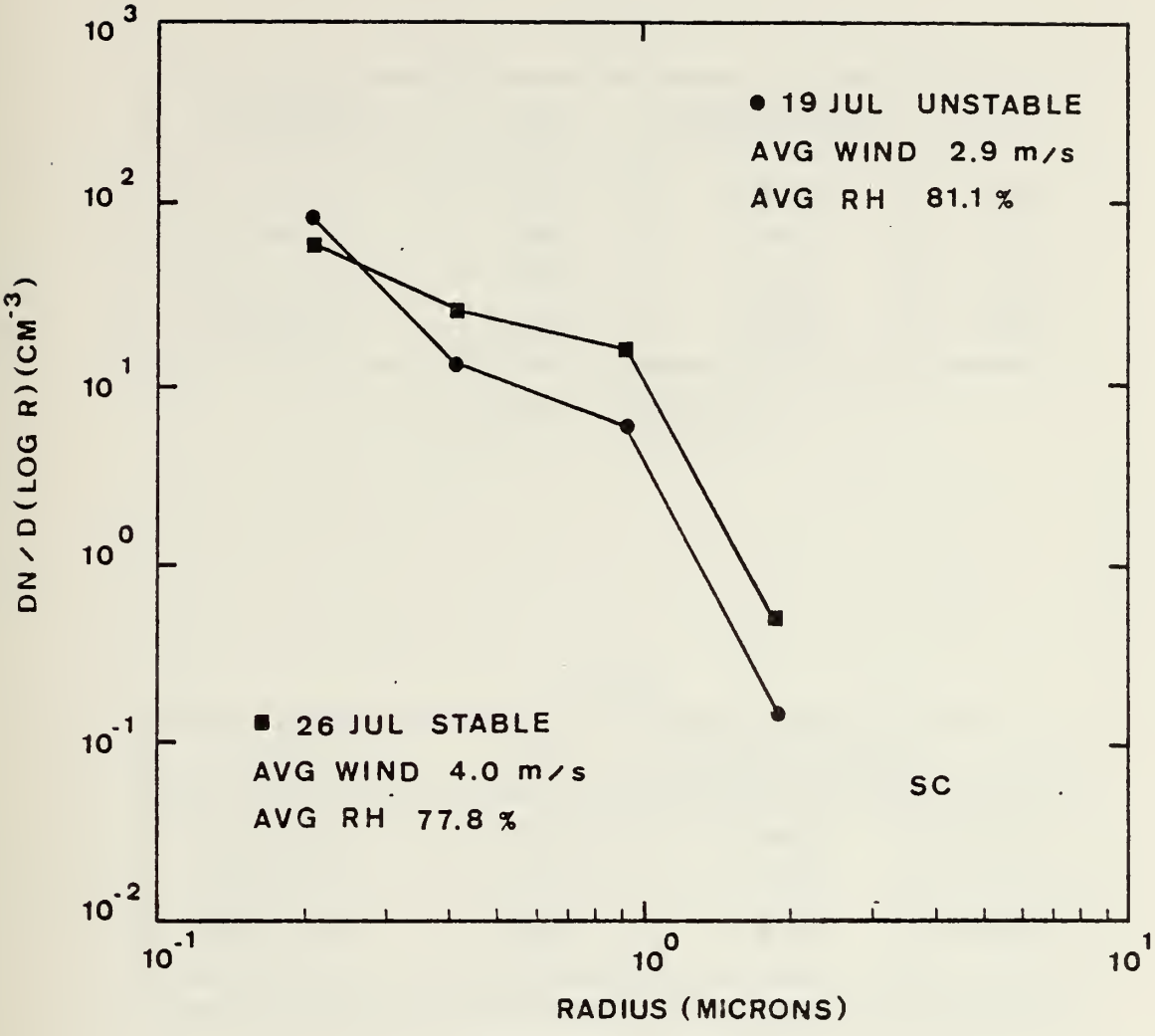

Figure 22. Average Size Distributions on 19 July and 26 July

SC

INTERVAL	RH	WIND SPEED	U_*
.15 – .30 μ	.814	–.205	.129
.30 – .60 μ	.837	–.184	.165
.60 – 1.5 μ	.792	–.110	.147
1.5 – 2.5 μ	–.104	–.049	.075

19 JUL UNSTABLE

SC

INTERVAL	RH	WIND SPEED	U_*
.15 – .30 μ	.610	–.395	–.372
.30 – .60 μ	.754	–.499	–.535
.60 – 1.5 μ	.835	–.615	–.634
1.5 – 2.5 μ	.355	–.413	–.273

26 JUL STABLE

Table III. Correlation Coefficients for 19 July and 26 July

level. The lower average wind speed associated with the unstable period does not allow for much sea-salt production. An unstable atmosphere can lead to convective processes which may vertically transport aerosols and create higher concentrations at an upper level as proposed by Ericksson (1959) and Toba (1965a & b). Hence, a decrease in the size distribution on 19 July is observed. This evidence gives credence to the possibility that friction velocity is a better indication of aerosol size distribution than wind speed. On both days the correlation of the concentration with humidity is lowest in the largest size interval. This relationship is most pronounced on the unstable days and may be explained by sedimentation due to mixing and resulting increased coalescence.

The averaged diurnal variations of wind speed, relative humidity, friction velocity, and aerosol concentration are shown in Figures 23, 24, and 25. Again the negative relationship of aerosols to wind speed and U_* in the size range of generally less than 1 μ is indicated. A satisfactory relationship with relative humidity is not evident and this is probably due to transport by a secondary circulation. A land-sea breeze type of effect could account for the observed decrease in concentration of the particles smaller than 1.5 μ. As the heating over the land generates an on-shore flow along the coast, the wind increases and persists through the afternoon. The average wind direction derived from the observations of five random days during the experiment is shown in Figure 26. A westerly wind is

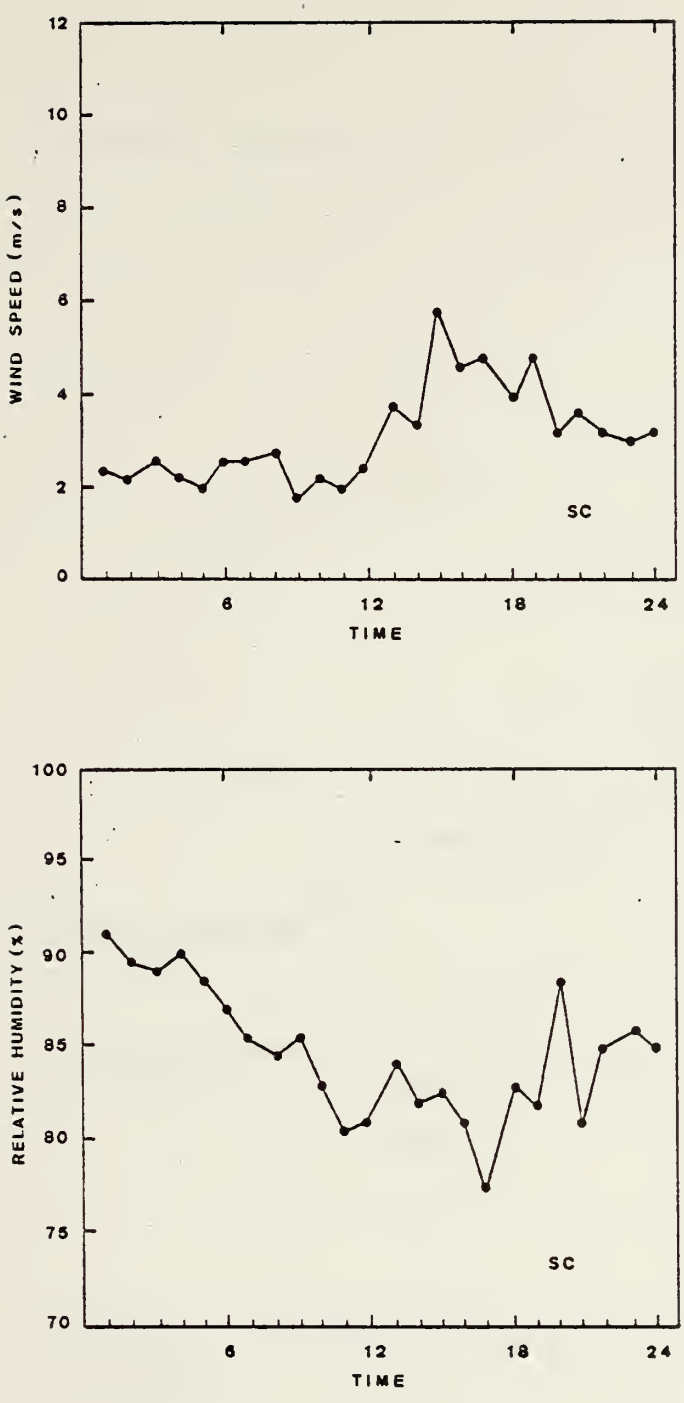

Figure 23. Average SC Diurnal Variations of Wind Speed and Relative Humidity

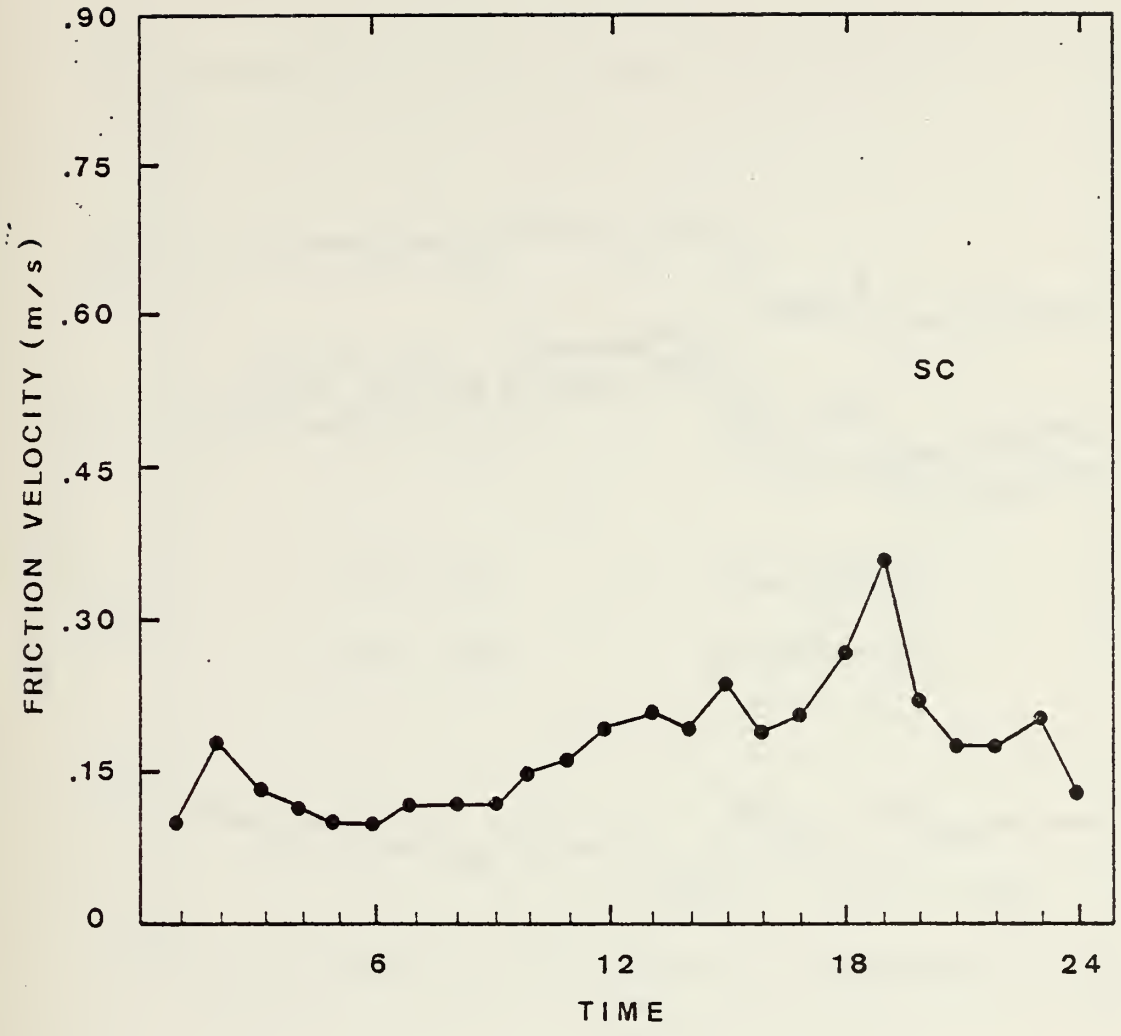

Figure 24. Average SC Diurnal Variation of Friction Velocity

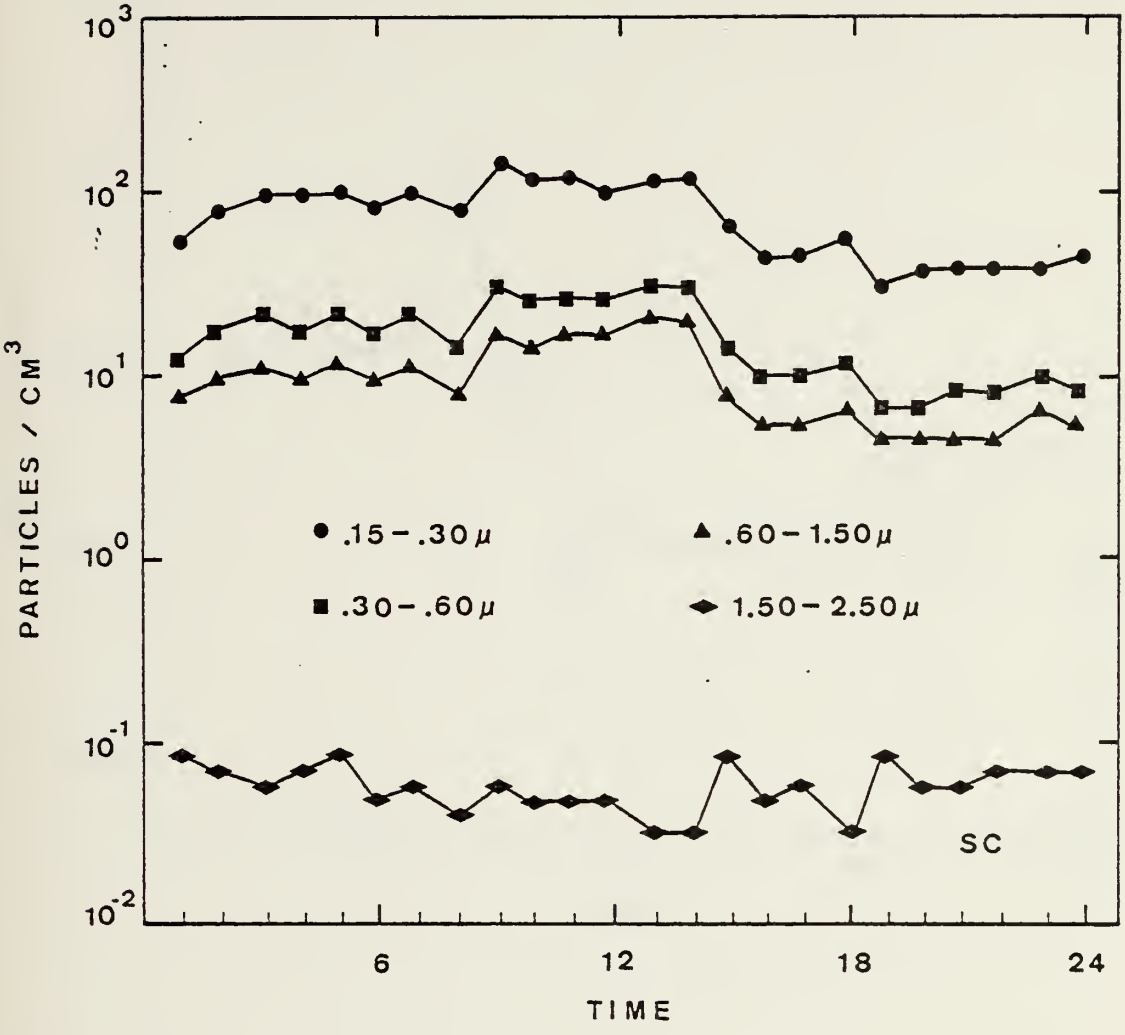

Figure 25. Average SC Diurnal Variations of Particle Concentrations

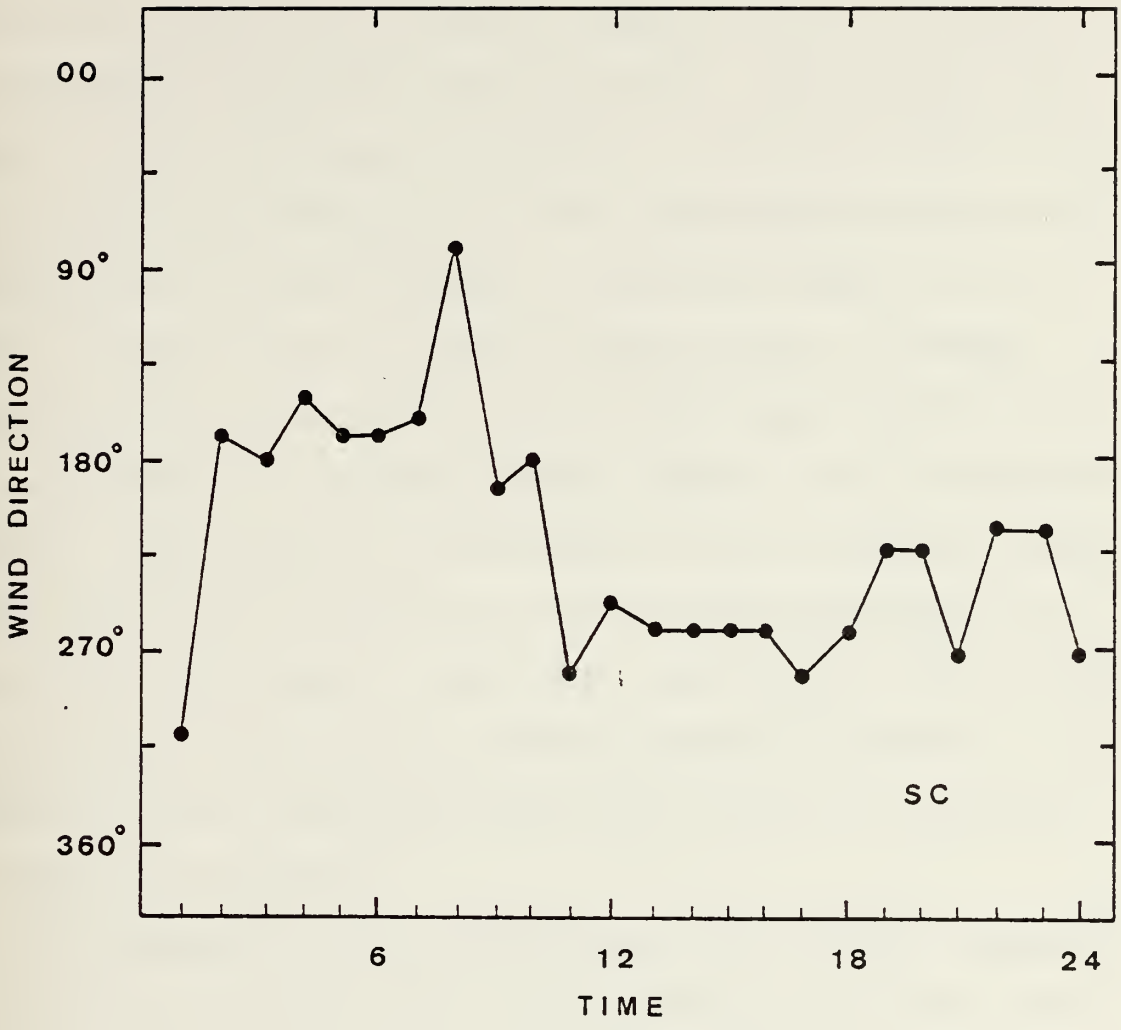

Figure 26. Average SC Wind Direction

seen to dominate during the peak wind periods. The decrease in the aerosol population may be explained by a horizontal divergence effect in the marine boundary layer as largest accelerations are found near the coast. The average size distributions displayed in Figure 27 reflect the decrease in the aerosol population due to this sub-synoptic circulation. Although the relative humidity increases slightly in the early evening hours, the smaller nuclei show a stronger relationship with the wind speed. This again implies that a large part of the coastal marine aerosol is of continental origin. The outflow of circulation aloft is probably responsible for the introduction of continental particulates to the marine environment. The minor peaks in the small particle concentration and also the somewhat greater increase in the large particles during the afternoon should be attributed to sea-salt production.

The Panama City (PC) observations more closely resembled a marine environment. The Aitken particle count was lower and averaged 2600 cm^{-3} while the distribution curve showed a marked change from the Southern California data. Winter time synoptic scale features predominate in this region of the Gulf Coast. Cold frontal passages and an accompanying influx of continental air into the Gulf of Mexico are frequent occurrences. Subsequent movement of the high pressure ridge into Florida and off its eastern seaboard provides the circulation which reestablishes moist southerly flow and return of the marine aerosol. Figure 28 provides the synoptic analyses for the period of the experiment. Stable

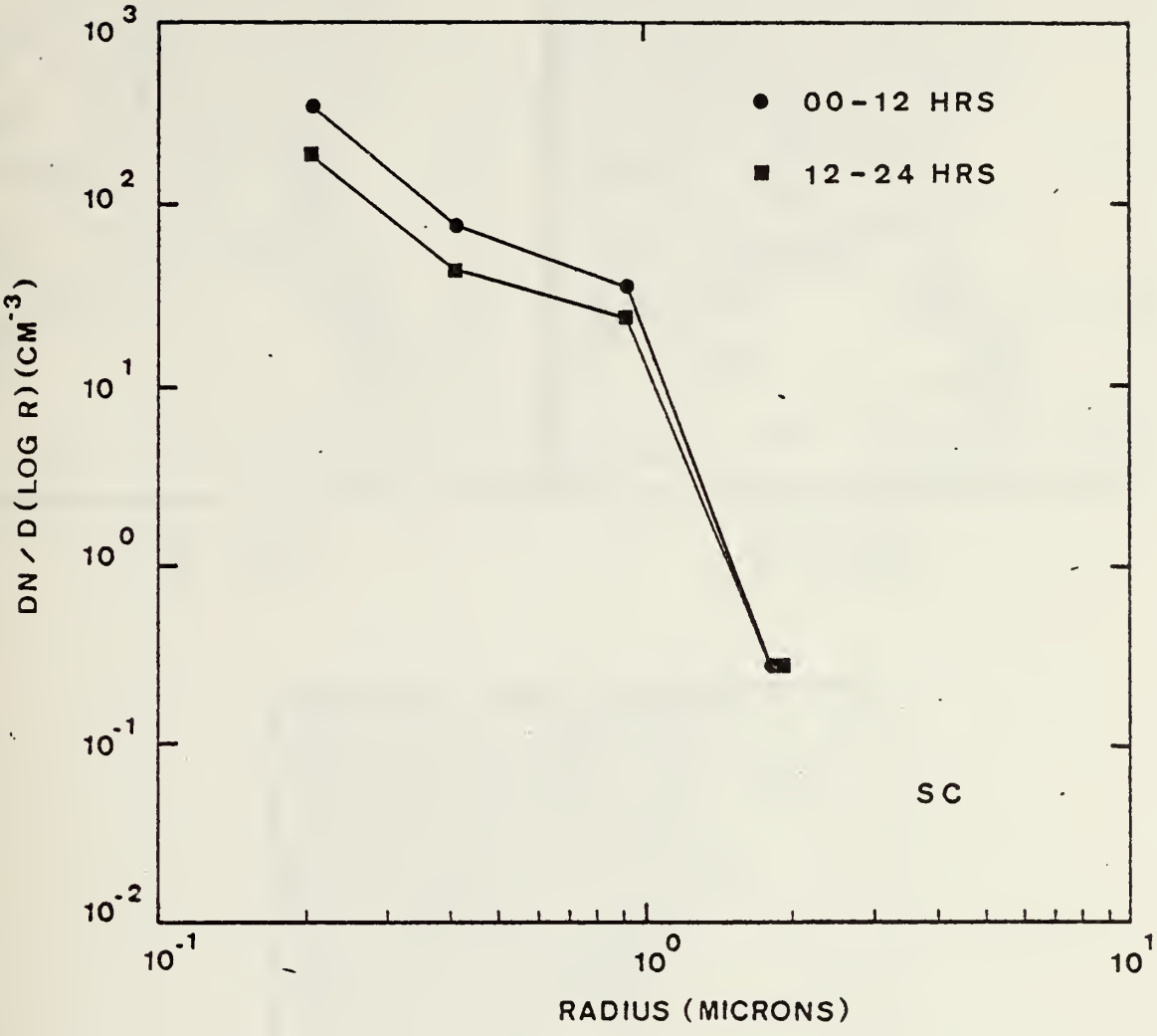

Figure 27. Average SC Diurnal Variation of the Aerosol Size Distribution

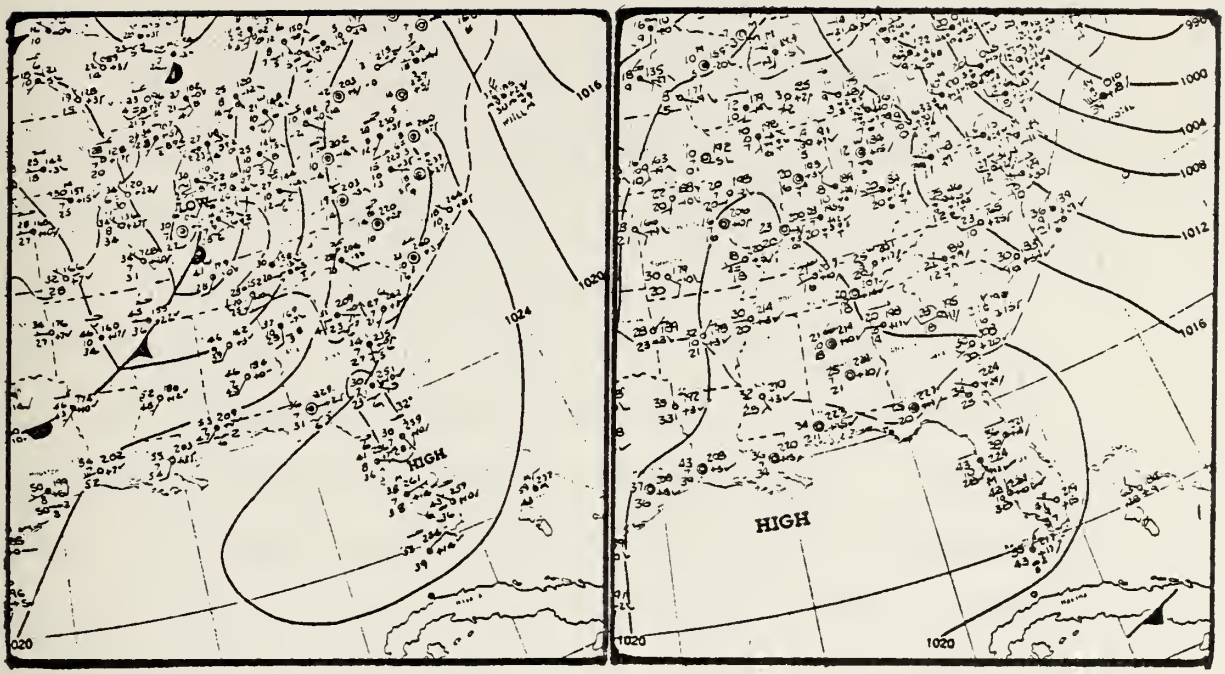

18 FEB

21 FEB

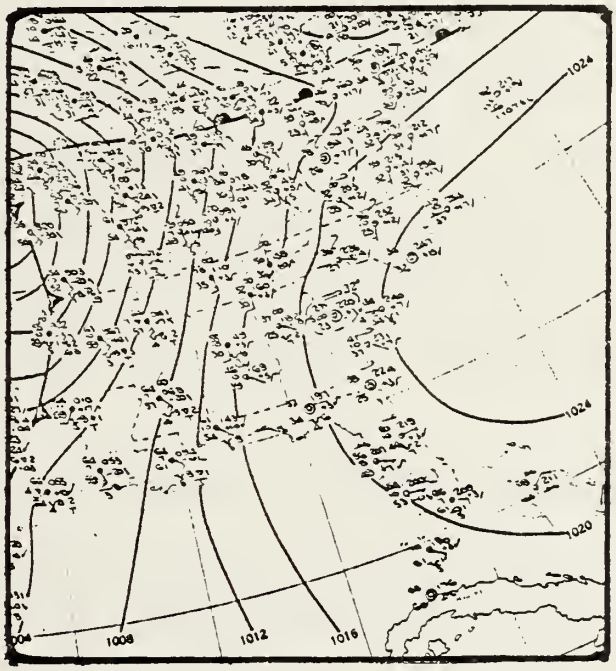

23 FEB

Figure 28. Synoptic Situation during the PC Experiment

conditions prevailed in the Panama City area at the beginning of the period; but, after frontal passage early on 20 February, south to southeasterly flow developed and persisted for the remainder of the experiment. The influx of this warm, moist air contributed a destabilizing effect in the lower levels of the marine boundary layer.

The average wind speed and relative humidity for PC were 8.4 m/sec and 71 percent, respectively. Fitzgerald's curve for these average conditions and the average aerosol distribution for the entire period are shown in Figure 29. Good agreement exists only for particle size range greater than .9 μ radius. The observed concentrations are approximately an order of magnitude lower than Fitzgerald's prediction for aerosols smaller than .5 μ radius. A significant aspect of the distribution is the positive slope observed between approximately .5 μ and 1 μ radius which appears to be the result of sea-salt production. Actually, good agreement is shown with Blifford's (1970) observation off the Pacific coast with respect to both slope and number concentration.

Plots showing the effect on the average distributions due to wind speed and relative humidity separately are shown in Figures 30 and 31. Relatively good correlations seem to exist between these parameters and the aerosol distributions. Correlation coefficients are presented in Table IV. The synoptic scale effects predominate over diurnal variations and wind speed and relative humidity are both positively correlated to the concentration. The highest correlation of

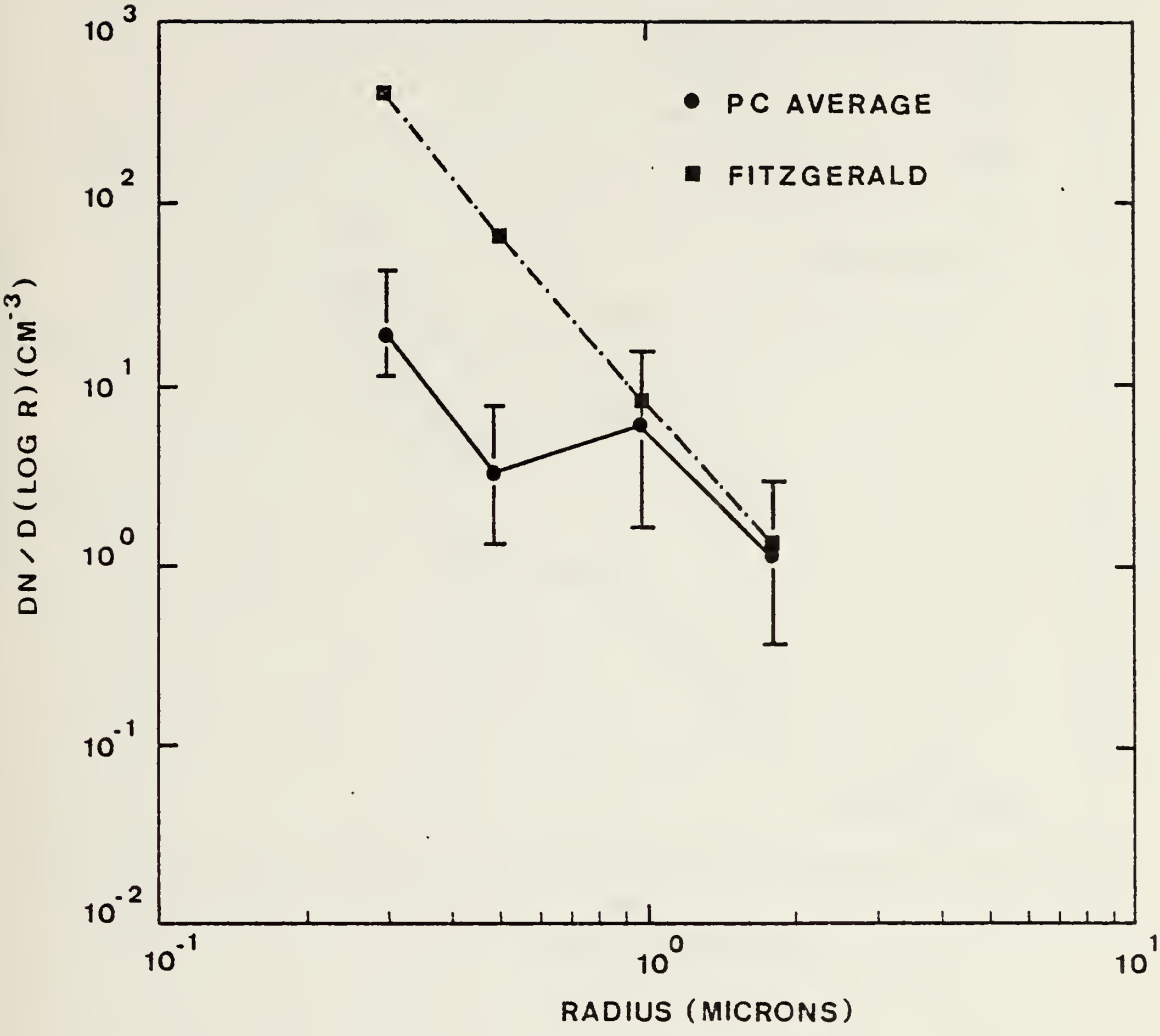

Figure 29. Average Aerosol Size Distribution for the PC Experiment and Distribution Predicted by Fitzgerald's Model

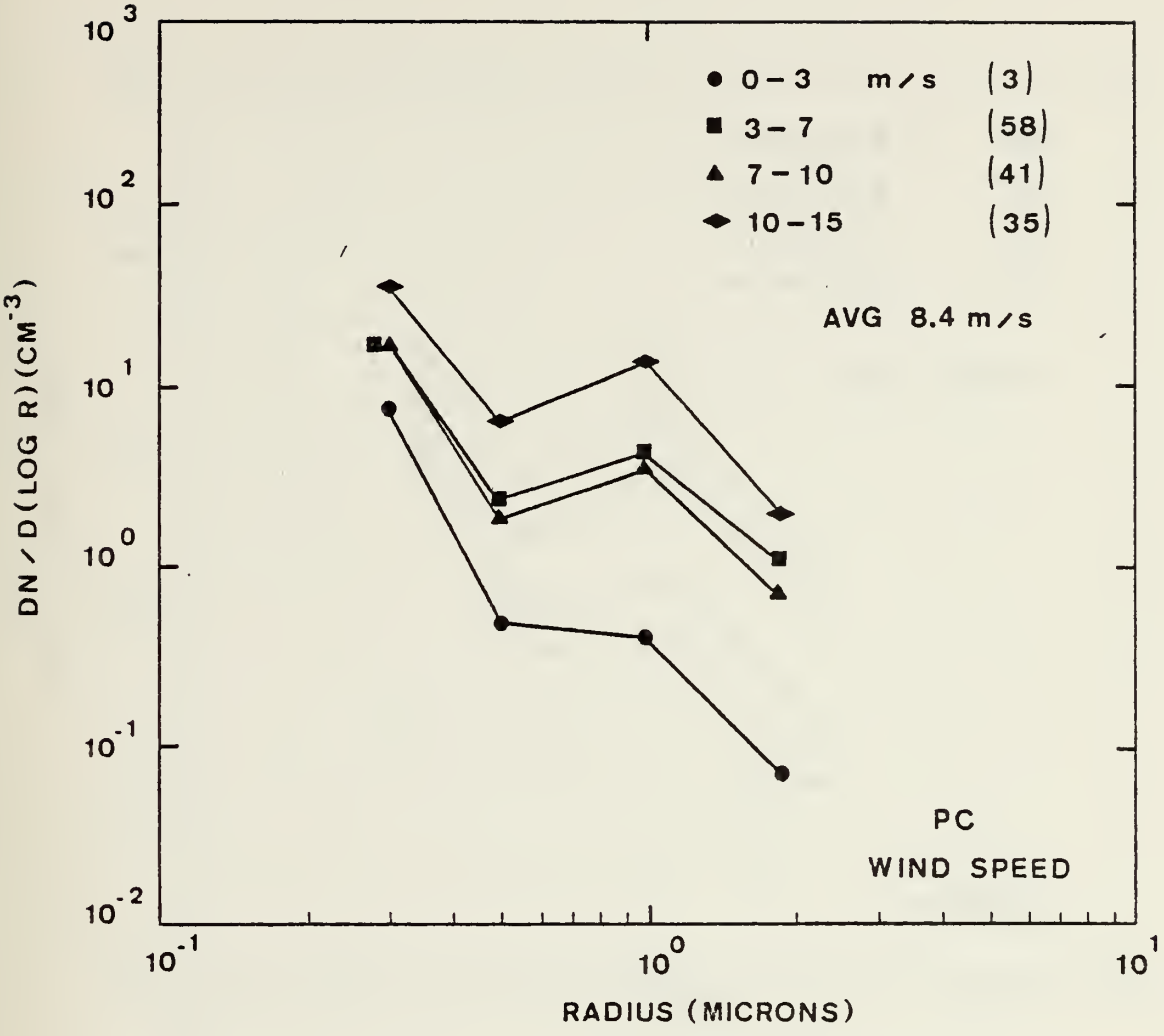

Figure 30. Variation of PC Size Distribution with Wind Speed

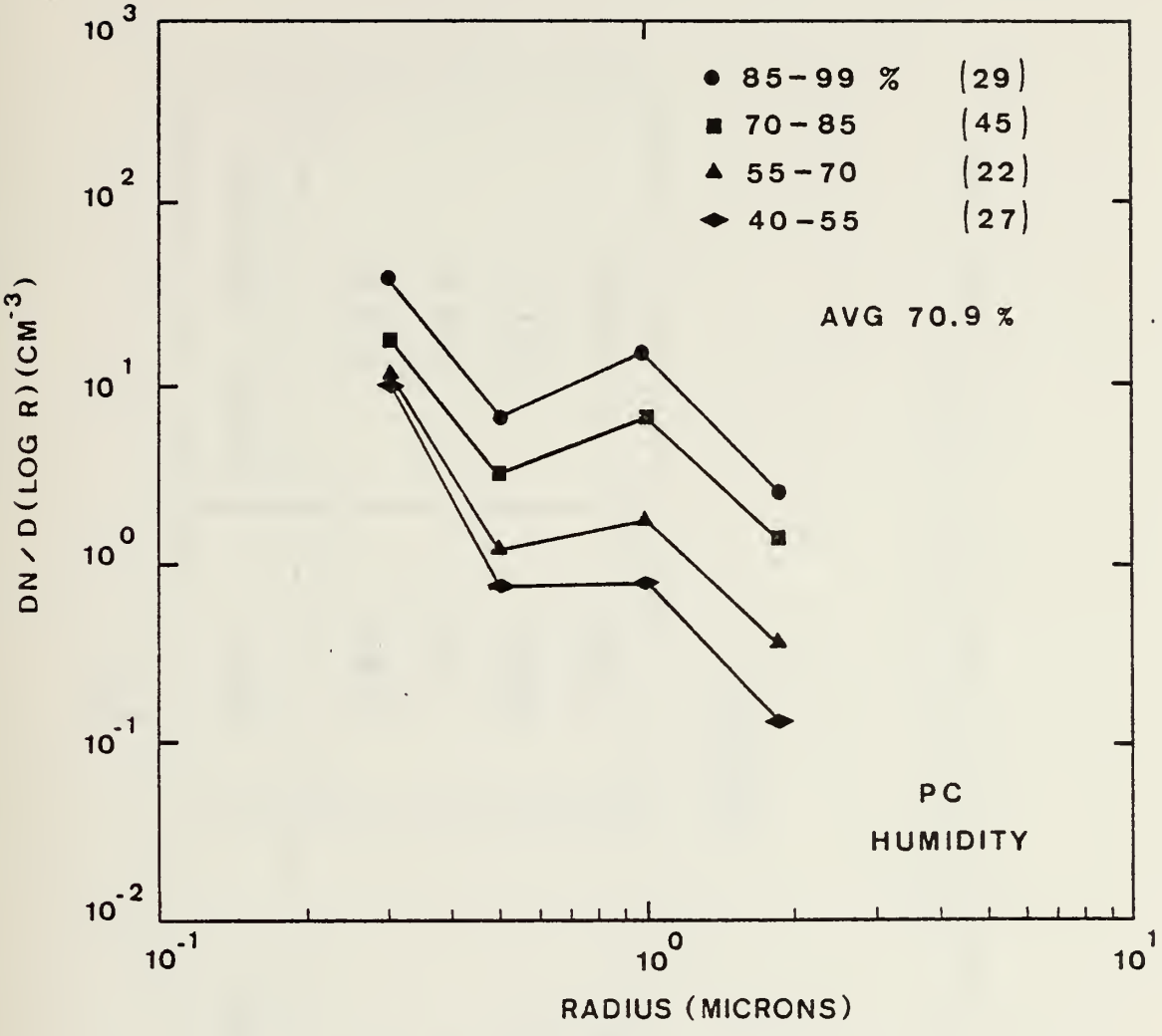

Figure 31. Variation of PC Size Distribution with Relative Humidity

PC

INTERVAL	RH	WIND SPEED
.25 – .35 μ	.620	.559
.35 – .70 μ	.726	.554
.70 – 1.5 μ	.654	.511
1.5 – 2.5 μ	.729	.442

TOTAL

Table IV. Correlation Coefficients for the PC Experiment

concentration to humidity at Panama City is witnessed in the 1.5 μ to 2.5 μ interval. This result may indicate that equilibrium tends to exist between production and sedimentation in this interval as hypothesized by Moore and Mason (1954). Disagreement exists in that the steeper negative slope is found during periods of strongest wind. The plot showing the effect of relative humidity on the size distributions results in small variations in the .25 μ - .35 μ interval. This probably indicates that the majority of these particles represent a mixture of continental and marine nuclei.

The stability influence was investigated by comparing observations on 18 February and 21 February. Temperature measurements at various levels on the platform made it possible to examine the lapse rates and determine the stability. The average distributions for these days grouped according to wind speed, and respective correlation coefficients are shown in Figures 32 and 33. The low humidities on 21 February resulted from the earlier intrusion of continental air, but southeast to southwest flow persisted most of the day. Although this trajectory helped to advect in warmer air, production of sea-salt dropped off as the wind decreased considerably below 7 m/sec. A much larger decrease is observed in the distribution curve on 21 February as compared to 18 February when the wind speed decreased below 7 m/sec. This agrees well with Moore's (1952) finding that the change in opacity is well marked during periods of low humidity. Also the decrease in the slope of the curve between .5 μ and

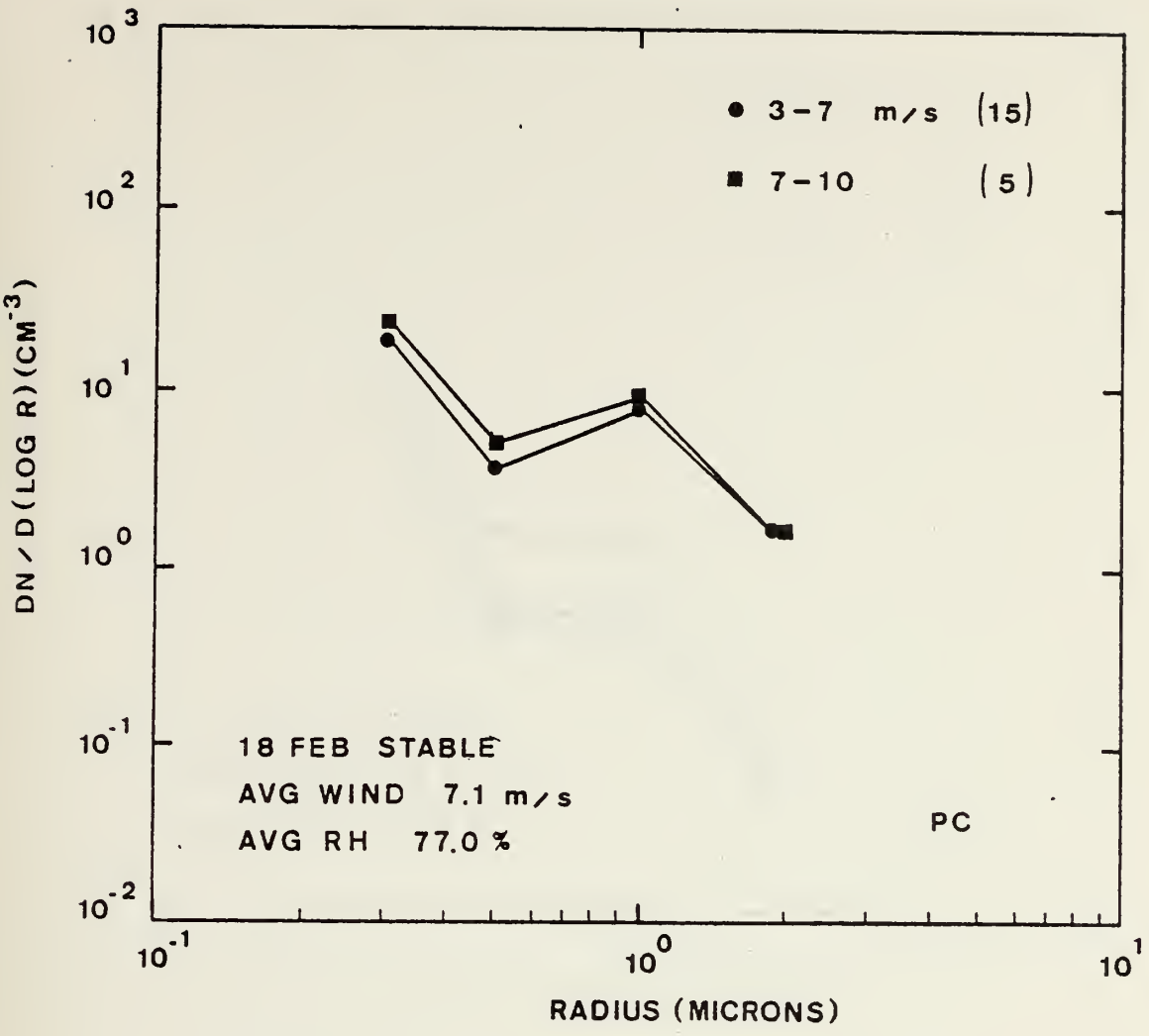

PC

INTERVAL	RH	WIND SPEED
.25-.35μ	.169	.065
.35-.70μ	.104	.334
.70-1.5μ	.279	.605
1.5-2.5μ	.385	.442

18 FEB STABLE

Figure 32. Correlation Coefficients and Variation of the Size Distribution with Wind Speed, 18 February

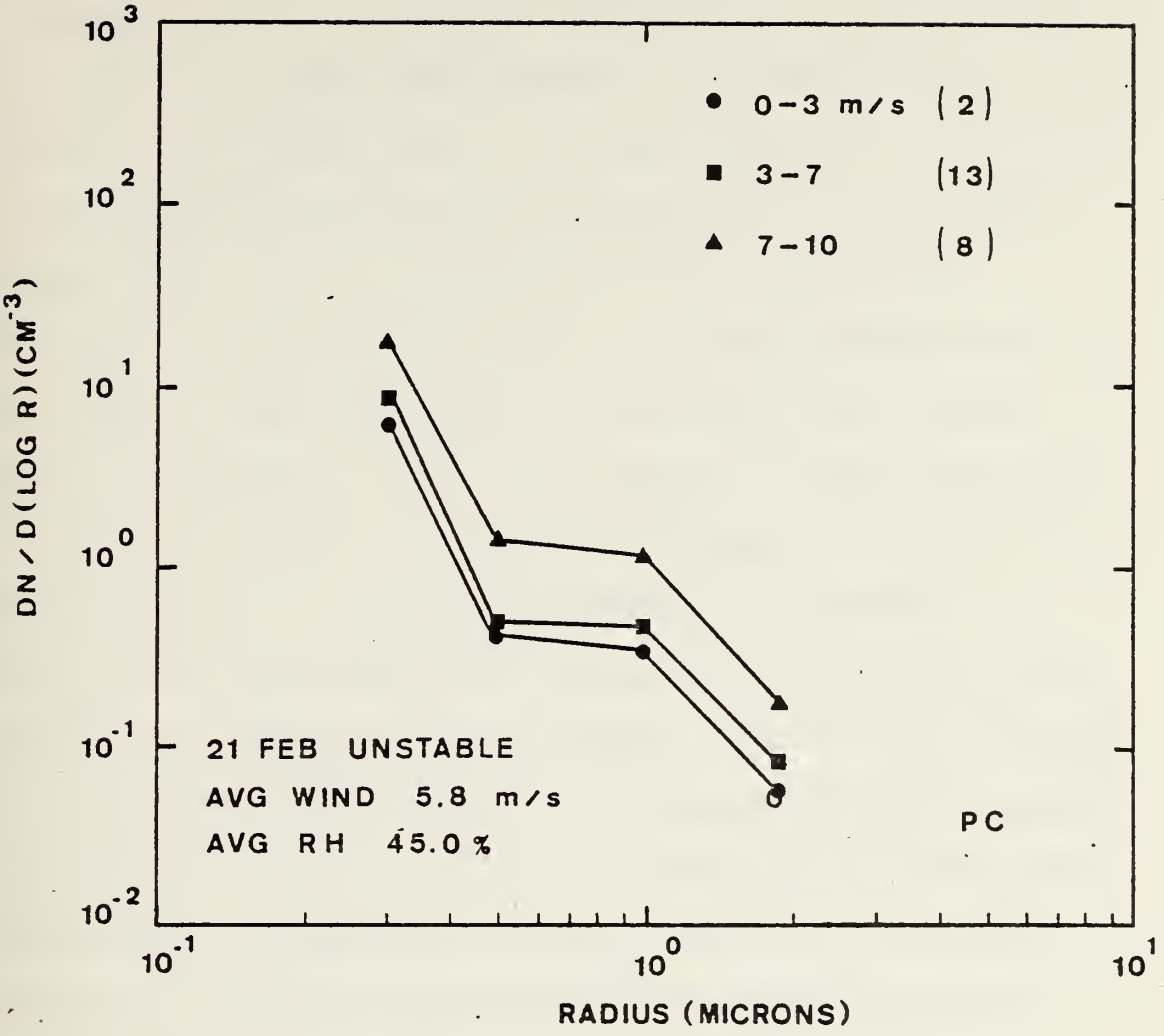

PC

INTERVAL	RH	WIND SPEED
.25-.35μ	.746	.615
.35-.70μ	.692	.651
.70-1.5μ	.558	.737
1.5-2.5μ	.253	.571

21 FEB UNSTABLE

Figure 33. Correlation Coefficients and Variation of the Size Distribution with Wind Speed, 21 February

1 μ appears to be a function of decreased relative humidity. This again reinforces the premise that sea-salt nuclei predominate in the size range above approximately .7 μ.

The correlation between concentration and wind speed for all size ranges is greatest on the unstable day. As with the SC data, this is consistent with momentum and diffusion theory. Again the small correlation with relative humidity exhibited by the larger nuclei is probable caused by growth and sedimentation in the absence of significant sea-salt production. When generation was occurring on 18 February, the large particles exhibited the largest correlations with humidity and wind speed. This stable stratification evidently was produced by a previous frontal passage and northerly flow of cold air and accompanying continental particulates. Therefore, a large portion of the aerosol at the beginning of the experiment may have been composed of non-hygroscopic material.

Figures 34 and 35 display the average diurnal changes in wind speed, relative humidity, and aerosol concentration. Again positive correlations are noted as relative humidity and wind speed, although containing quite a bit of scatter, tend to vary accordingly. Of most significance would be the obviously high concentration of droplets in the .7 μ - 1.5 μ range. Noting that the average wind seldom went below 7 m/sec, this would indicate that sea-salt nuclei production is greatest in this size range. A diurnal representation of the average aerosol distribution is presented in Figure 36.

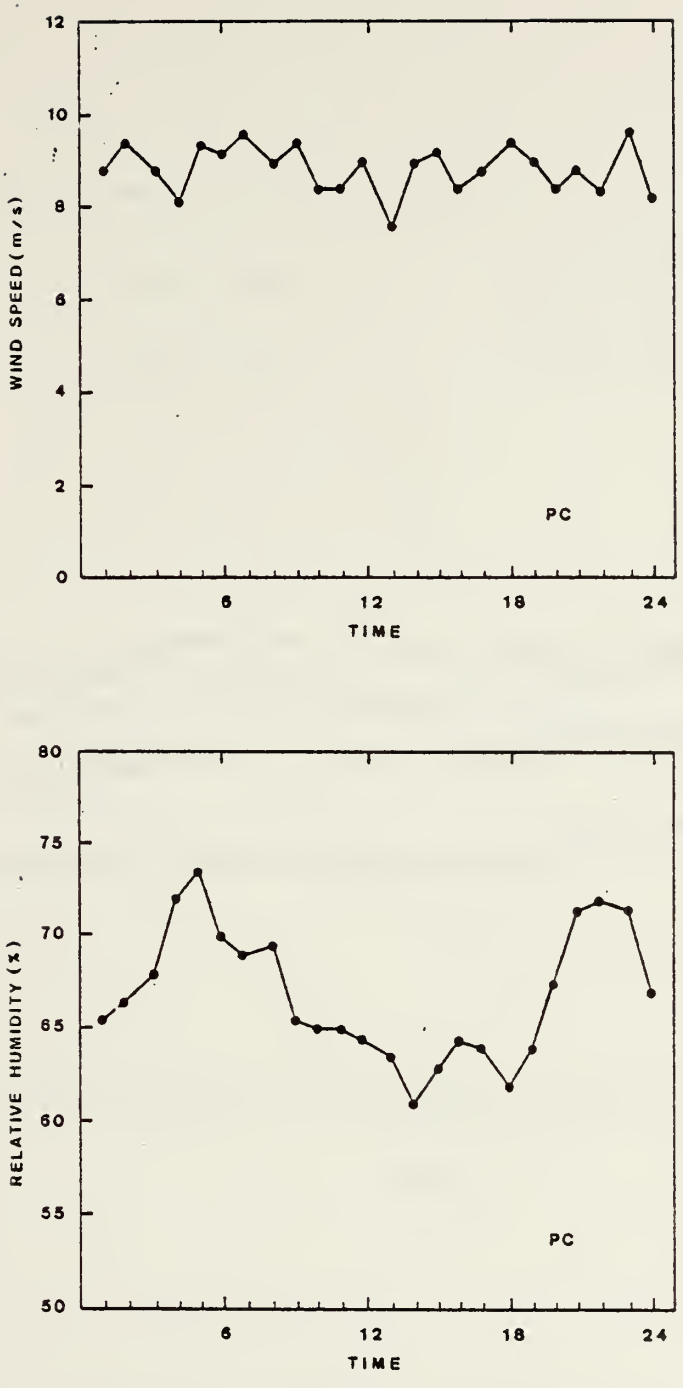

Figure 34. Average PC Diurnal Variations of Wind Speed and Relative Humidity

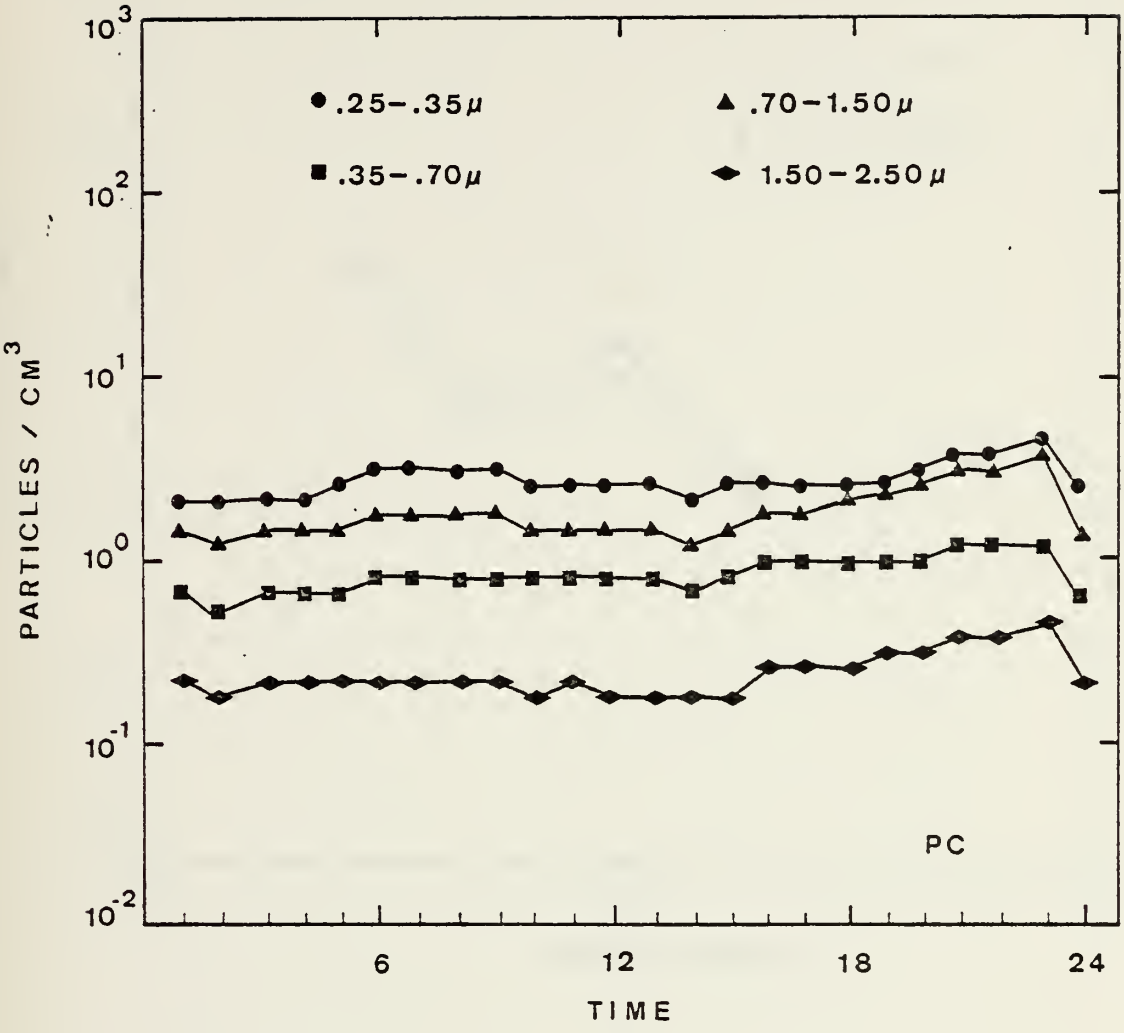

Figure 35. Average PC Diurnal Variations of Particle Concentrations

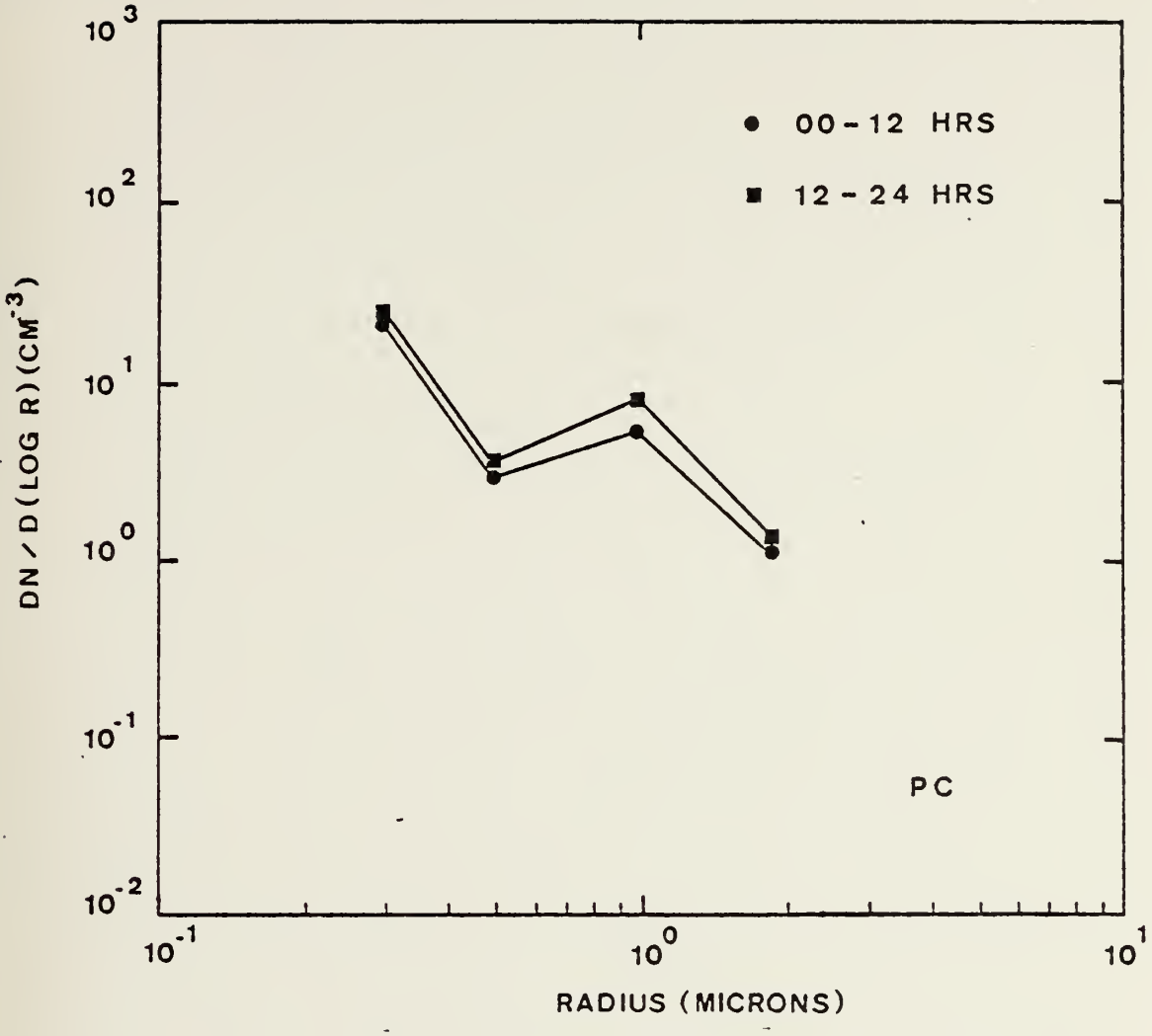

Figure 36. Average PC Diurnal Variation of the Aerosol Size Distribution

Any transport of aerosols due to a land-sea breeze effect should be ruled out as a satisfactory relationship does not seem to exist.

VII. CONCLUSIONS

The coastal marine aerosol is shown to be a highly variable function of the interaction between synoptic and mesoscale processes. Important meteorological parameters such as wind speed, relative humidity, and stability are dependent upon secondary circulations between land and sea in the absence of large scale forcing.

The minimum concentration in the size distribution curves at .4 μ - .5 μ radius may indicate that this size is indeed the transition zone between the two bubble bursting sea-salt producing mechanisms. Since the slope on either side of this zone is steeper during the Panama City experiment, wind speeds of greater than 7 m/sec result in the generation of sea-salt particles larger than .25 μ radius. Sedimentation of particles larger than 1.5 μ appears to be most significant during periods of low wind speed. During strong winds a state of equilibrium between sedimentation and production exists for these larger particles.

Relative humidity variations have the largest effect on the aerosol size distribution in the absence of sea-salt production. The concentration of the coastal marine aerosol is most sensitive to wind speed effects at low relative humidity. Friction velocity seems to be a better indication of the aerosol size distribution than wind speed under unstable atmospheric conditions. Also during light wind

periods, instability appears to result in a decrease in concentration at the observation height. Enhanced diffusion during periods of sea-salt production causes vertical transport of sea-salt from the sea surface and an increase in concentration.

Any effect of surface organic film possibly suppressing the production of small sea-salt particles could not be examined because of the absence of significant generation off the Southern California coast.

Table V, Panama City Data

DATE & TIME	RH	WIND DIR & SPEED	AITKEN CON	# PARTICLES / 2.8 L	>.5	>.7	>1.4	>3.0	>5.0
18 0	77	28015	3000	21075	11206	7935	1287	200	
18 100	68	28018	2300	21791	12419	8953	1324	216	
18 200	72	27517	2000	18261	10588	7662	1147	179	
18 300	72	28014	0	22634	13397	9792	1598	308	
18 400	72	28514	0	23305	13914	10391	1644	265	
18 500	83	29015	1500	23266	13930	10350	1588	270	
18 600	83	28014	1600	24627	14956	11146	1701	294	
18 700	76	28518	1800	25487	15548	11471	1570	228	
18 800	78	28519	1800	24018	14461	10607	1450	220	
18 900	73	28017	1600	23908	14357	10543	1491	225	
18 1000	70	27515	0	22752	13351	9447	1317	190	
18 1100	73	25015	0	21002	11973	8285	1161	174	
18 1200	73	26514	1700	19602	10473	7014	1067	144	
18 1300	73	26018	1600	18490	8917	5471	879	109	
18 1500	74	25013	2100	17104	8210	5095	722	76	
18 1600	84	28011	1900	19002	10300	6921	1068	127	
18 1700	78	28514	2000	18102	10248	7048	1117	158	
18 2100	66	27014	1800	23647	13953	10385	1685	290	
18 2200	84	27514	1700	23440	13872	10274	1655	299	
18 2300	84	27015	1700	22644	13309	9635	1447	240	
19 0	81	26516	1600	22648	13433	9744	1480	257	
19 100	82	28018	1500	20363	11832	8320	1236	209	
19 200	83	28017	0	18567	10848	7698	1163	180	
19 300	84	28015	0	20337	11916	8591	1314	203	
19 400	84	28013	0	20082	11917	8739	1486	220	
19 500	85	28013	0	17003	9872	7170	1245	212	
19 600	86	28013	1600	15437	8631	6196	1047	174	
19 700	86	27512	1500	15227	8438	6035	1014	194	
19 800	87	27013	1500	13569	7784	5624	1002	190	
19 400	87	26512	3200	12605	6852	4832	804	126	
19 1000	86	26512	1350	12267	6664	4695	781	133	
19 1100	85	26510	0	12084	6339	4514	716	92	
19 1200	83	25011	0	10293	5103	3402	567	84	
19 1300	82	26511	1300	10089	4854	3057	489	65	
19 1400	77	25512	1500	11280	5547	3588	592	73	

DATE & TIME	RH	WIND DIR & SPEED	AITKEN CON	# PARTICLES / 2.8 L	>.5	>.7	>1.4	>3.0	>5.0
19 1500	77	27516	1400		11953	6074	2959	621	75
19 1600	74	25015	1900		13707	7262	4518	818	119
19 1700	81	24014	1600		13113	6951	4792	822	115
19 1800	83	24014	1500		14767	8359	6040	1100	191
19 1900	86	24514	2400		15396	8762	6423	1134	196
19 2000	85	25014	3900		16318	8251	5921	1060	184
19 2100	81	27015	5000		22721	9815	6807	1206	199
19 2200	86	28512	5200		27510	12120	8448	1448	240
20 200	69	35028	0		9030	2810	1640	201	37
20 300	66	35025	0		8603	2198	1196	160	23
20 400	62	35523	0		6091	1542	822	82	11
20 500	58	35021	8000		8187	1598	1067	139	19
20 600	51	35319	0		9283	2094	1125	142	21
20 700	51	35519	0		10768	2421	1193	138	16
20 800	51	35018	0		8003	1788	878	93	19
20 900	58	33516	0		7142	1327	666	59	12
20 1000	45	34017	0		6425	1375	681	57	8
20 1100	37	32019	0		5229	1248	736	125	36
20 1200	35	31521	0		4356	972	566	77	25
20 1300	35	31015	0		3806	1027	637	135	35
20 1400	30	31516	0		3155	871	536	89	18
20 1500	31	30020	0		2532	680	416	60	23
20 1600	32	30517	0		2671	712	457	74	16
20 1700	26	30515	0		4768	934	534	68	17
20 1800	24	32013	0		4334	1005	569	78	14
20 1900	29	35012	0		3243	998	684	167	54
20 2000	33	32010	0		3482	893	530	92	22
20 2100	49	29017	0		7045	2528	1586	260	51
20 2200	49	28518	0		6983	2076	1238	169	23
20 2300	49	33026	0		9442	2659	1636	254	52
21 0	44	33021	0		9384	2823	1667	267	74
21 100	42	32518	2700		7582	2674	1691	304	79
21 200	39	35016	2700		5155	1323	724	64	11
21 300	44	518	0		5417	715	278	5	1
21 400	49	1518	0		8835	1702	821	49	7

DATE & TIME	RH	WIND DIR & SPEED	AITKEN CON	# PARTICLES / 2.8 L	>.5	>.7	>1.4	>3.0	>5.0
21 500	57	5017	2400	16227	3181	1482	135	29	
21 600	51	6516	2200	14496	3144	1565	171	42	
21 700	51	8516	2200	15791	3463	1508	104	11	
21 800	52	10511	3300	10451	2086	963	57	8	
21 900	47	135 9	5000	6777	1389	688	64	9	
21 1000	42	130 8	0	5794	1212	633	67	12	
21 1100	45	155 6	0	4743	988	511	56	6	
21 1200	42	175 6	8000	3590	910	494	62	10	
21 1300	37	215 7	9000	2672	567	300	35	7	
21 1400	40	205 8	7000	2650	546	324	40	4	
21 1500	40	240 8	0	2469	502	268	33	2	
21 1600	39	240 9	0	2643	597	310	39	7	
21 1700	38	24510	4500	2585	678	371	41	11	
21 1800	43	24010	4000	3040	702	402	55	7	
21 1900	43	22510	2900	3282	808	451	64	10	
21 2000	49	23511	3100	3133	780	435	69	10	
21 2100	47	22510	2800	3124	757	467	76	8	
21 2200	47	21510	3000	3321	888	520	71	10	
21 2300	48	20010	3000	3396	880	492	73	11	
22 0	48	200 9	2800	3404	896	485	71	11	
22 100	55	18011	2700	3360	903	520	79	11	
22 200	55	16511	2200	2902	846	510	89	6	
22 300	59	14513	0	3556	1218	766	112	7	
22 400	64	14014	0	3735	1478	971	135	18	
22 500	71	13517	2000	5366	2287	1517	256	32	
22 600	68	14019	2000	6182	2747	1908	278	42	
22 700	66	14019	2000	6688	3031	2049	341	61	
22 800	66	14021	2000	7297	3365	2262	311	54	
22 900	61	13822	1800	7299	3345	2223	298	30	
22 1000	62	13522	2100	6784	3129	2050	278	28	
22 1100	65	13522	0	8511	4341	3010	402	61	
22 1200	69	13522	2300	8865	3906	2565	336	34	
22 1300	66	13522	2500	9368	4203	2663	375	45	
22 1400	66	13822	3600	8305	3451	2225	333	34	
22 1500	66	13322	0	8253	3500	2207	335	38	

DATE & TIME	RH	WIND DIR & SPEED	AITKEN CON	# PARTICLES / 2.8 L	>.5	>.7	>1.4	>3.0	>5.0
22 1600	65	14518	2400		8193	3551	2283	326	34
22 1700	71	13025	3200		9455	4276	2846	443	49
22 1800	70	12026	3000		9013	3928	2632	332	44
22 1900	70	11826	3000		10166	4562	3072	421	56
22 2000	76	14021	2500		10704	4593	3058	450	60
22 2100	73	15022	3300		8087	3483	2251	273	21
22 2200	73	13817	2000		8393	4419	3067	508	82
22 2300	82	12815	1700		10198	5447	3862	678	111
23 0	85	12018	2000		11639	6411	4566	678	87
23 100	80	11821	1700		12617	7048	5002	686	86
23 200	82	12522	2000		14337	8001	5818	839	129
23 300	84	13018	0		17257	9785	7192	1125	154
23 400	86	11518	0		18069	10235	7559	1076	191
23 500	88	11027	3500		18055	9843	7041	901	116
23 600	82	11527	2800		24855	14118	9970	1180	158
23 700	82	11028	3200		27584	15405	10982	1297	179
23 800	83	11024	3100		34453	18582	13313	1685	209
23 900	88	11028	3300		34011	18410	13031	1563	170
23 1000	86	11525	0		31144	16629	11121	1223	102
23 1100	86	11027	2700		36249	19615	13208	1332	107
23 1200	86	11521	2600		36875	20600	13936	1504	132
23 1300	89	13026	2400		37036	21113	14636	1696	188
23 1400	91	12529	2400		37751	21301	14593	1712	145
23 1500	91	11528	1800		41249	22854	15329	1493	134
23 1600	92	12829	1700		48270	28627	20153	2165	254
23 1700	91	11526	1600		48641	29137	20620	2117	208
23 1800	91	12528	1800		52317	31873	23169	2510	275
23 1900	91	14025	1700		60162	37378	28007	3312	505
23 2000	94	13325	1500		68059	42388	32516	4167	690
23 2100	94	14026	1300		70670	44713	34659	3822	518
23 2200	94	14528	0		75264	46227	36507	3174	281
23 2300	94	15528	1200		95924	56409	45316	5071	516

Table VI. Southern California Data

DATE & TIME	RH	REL WIND DIR & SPD	SHIPS HEAD & SPD	AITKEN CON	# PARTICLES / .28 L	>.3	>.6	>1.2	>3.0	>5.0
19 C	85	287 3	270 0	3000		12344	2531	933	10	0
19 100	92	290 1	270 0	1500		14239	2526	896	10	0
19 200	87	260 1	270 0	1700		15632	2975	1039	5	0
19 300	85	192 1	270 0	3500		12690	2660	995	11	0
19 400	85	18010	180 9	0		13914	2475	797	10	0
19 500	85	18010	180 9	0		14444	2485	841	6	0
19 600	80	340 7	140 9	0		6461	1459	578	7	0
19 700	82	19 6	140 9	0		6028	1371	550	10	0
19 800	81	360 9	205 9	0		9612	1673	624	9	0
19 1000	77	215 1	353 2	0		9261	1509	545	6	0
19 1100	76	172 9	175 9	3800		6793	1305	479	6	0
19 1120	76	172 9	175 9	0		7046	1429	565	11	0
19 1130	76	172 9	175 9	8500		6785	1321	529	10	0
19 1140	76	172 2	155 2	2200		6530	1290	495	12	0
19 1150	76	172 2	155 2	3000		6374	1321	489	10	0
19 1200	74	168 3	168 2	1300		6215	1357	579	14	0
19 1300	75	168 3	168 2	1200		6173	1291	503	12	0
19 1400	78	168 3	168 2	1500		6215	1304	456	5	0
19 1430	78	234 7	254 0	2900		6760	1466	583	22	0
19 1600	78	305 6	317 0	2100		8352	1618	585	7	0
19 1700	80	284 2	274 0	1300		6632	1340	504	12	0
19 1800	82	190 1	133 9	1200		7095	1491	575	14	0
19 2000	86	220 8	167 9	1150		8226	1658	610	10	0
19 2100	86	175 5	147 9	1800		11798	2088	728	5	0
19 2200	83	160 1	147 0	1400		11950	2139	723	16	0
19 2300	80	315 0	147 0	0		11620	2033	689	12	0
20 C	82	183 1	147 0	0		9526	1780	643	7	0
20 100	82	67 2	147 0	0		9986	1747	637	11	0
20 200	84	290 2	147 0	0		11695	1912	662	10	0
20 300	82	90 4	147 0	0		19871	4111	1473	8	0
20 400	84	280 5	0 0	0		23000	4668	1635	8	0
20 500	84	280 4	0 0	0		22081	4189	1431	5	0
20 555	84	270 5	0 0	5100		23114	4664	1628	8	0
20 610	84	270 3	0 0	8000		24115	4936	1784	5	0
20 625	84	270 3	0 0	4800		25023	5273	1922	8	0

DATE & TIME	RH	REL WIND DIR & SPD	SHIPS HEAD & SPD	AITKEN CON	# PARTICLES / .28 L	>.3	>.6	>1.2	>3.0	>5.0
20 650	84	270 3	0 0	0		23370	4879	1707	6	0
20 700	82	285 5	0 0	2400		23558	5028	1761	8	0
20 710	82	285 5	0 0	1950		22378	4658	1654	8	0
20 720	82	305 2	0 0	2700		21453	4445	1564	3	0
20 740	82	310 1	0 0	6000		22713	4723	1725	7	0
20 750	82	240 1	0 0	2400		21528	4536	1665	5	0
20 800	82	240 1	0 0	2200		22292	4675	1690	7	0
20 820	82	230 3	0 0	3000		24133	4141	1525	10	0
20 835	82	315 5	345 9	3900		22244	4640	1637	9	0
20 905	85	340 7	342 9	2900		22825	4953	1835	12	0
20 1000	82	310 8	350 9	1650		23006	5059	1865	14	0
20 1100	76	20 4	343 9	5500		13184	2310	793	7	0
20 1200	78	325 3	340 9	3600		12649	2228	733	5	0
20 1300	79	310 6	332 9	2500		14505	2066	629	6	0
20 1400	80	280 2	0 0	1600		15433	1917	550	3	0
20 1730	78	255 3	0 0	0		19117	3968	1393	7	0
20 1730	81	27510	350 0	9200		20619	4238	1448	8	0
20 1815	81	27510	350 0	0		19965	4032	1371	1	0
20 1900	86	27014	272 4	5800		21875	4718	1653	4	0
20 2005	87	27510	270 5	7000		26296	5768	2040	10	0
20 2050	85	280 5	0 0	5100		29881	6759	2438	7	0
20 2200	89	280 2	0 0	1900		27050	6880	2616	16	0
20 2300	88	300 3	0 0	3100		67724	20710	8710	16	0
21 0	93	330 7	360 9	2900		32913	8312	3119	14	0
21 100	94	305 2	0 0	4100		45895	12409	4761	5	0
21 200	95	225 2	265 9	0		51710	14480	5790	5	0
21 300	97	135 4	0 0	4400		55620	17960	7350	3	0
21 345	93	100 5	100 2	0		46050	12860	5264	5	0
21 500	90	125 2	0 0	5000		57565	16326	6641	19	0
21 545	90	160 2	0 0	5000		38950	9370	3548	17	0
21 645	87	170 1	0 0	2600		25425	5767	2250	16	0
21 800	87	170 1	0 0	0		34360	7496	2685	10	0
21 900	85	30 6	360 7	0		37857	7756	2730	15	0
21 1000	87	20 5	360 9	0		87734	25760	10098	15	0
21 1115	90	270 5	0 0	8200		98150	32021	13122	15	0

DATE & TIME	RH	REL WIND DIR & SPD	SHIPS HEAD & SPD	AITKEN CON	# PARTICLES / .28 L	>.3	>.6	>1.2	>3.0	>5.0
21 1215	90	260 8	0 0	7600	107112	36992	15930	11	0	
21 1300	90	260 16	265 5	5000	110540	39506	16729	9	0	
21 1400	90	274 16	254 6	7300	116775	37650	16290	1	0	
21 1445	87	280 14	0 0	21000	65554	16927	6258	5	0	
21 1600	85	260 12	0 0	4200	31756	7017	2589	13	0	
21 1700	86	270 9	0 0	4300	11364	3261	1257	14	0	
21 1800	85	265 9	0 0	9500	6360	2645	1179	17	0	
21 1925	82	250 6	0 0	6400	5863	2685	1230	30	0	
21 2010	85	225 7	0 0	5000	6259	2869	1307	21	0	
21 2115	84	295 1	0 0	5300	6557	3069	1502	28	0	
21 2200	88	80 9	53 9	4700	6587	2943	1464	25	0	
21 2300	94	100 1	0 0	4800	8985	3256	1491	21	0	
21 2315	94	100 1	0 0	4800	8739	3106	1416	16	0	
21 2325	94	15 8	360 9	5200	11636	3648	1570	24	0	
22 30	93	10 1	0 0	5600	10065	3569	1474	21	0	
22 100	91	20 1	0 0	5200	9586	3214	1418	18	0	
22 130	91	145 9	165 9	9000	12750	3889	1703	35	0	
22 140	91	145 9	165 9	16500	34751	7800	2960	18	0	
22 150	90	145 9	160 9	14500	58358	13095	4711	11	0	
22 200	90	145 9	160 9	19000	72729	17835	6563	17	0	
22 215	90	180 1	0 0	7300	50905	11661	4030	16	0	
22 230	92	180 1	0 0	10000	61164	14380	5195	16	0	
22 245	92	95 6	0 0	14000	68500	16653	5900	14	0	
22 300	94	95 6	25 9	11000	65880	15400	5500	14	0	
22 315	94	65 8	25 9	28000	72405	17859	6529	12	0	
22 330	93	122 3	0 0	27000	70800	16380	5523	16	0	
22 345	93	122 3	0 0	27000	57280	12460	4100	10	0	
22 355	92	300 5	267 9	19000	42050	8785	2657	27	0	
22 415	92	15 1	0 0	16000	30589	7094	2250	19	0	
22 445	92	15 1	0 0	0	73900	18800	7060	14	0	
22 515	95	120 3	0 0	21000	74348	19837	7487	18	0	
22 600	95	130 9	138 9	5500	64051	16194	6190	15	1	
22 645	95	10 7	360 9	9000	78139	20548	7623	10	0	
22 715	95	20 1	0 0	16000	100065	25740	11800	11	0	
22 800	93	20 1	0 0	9600	81079	21612	7759	12	0	

DATE & TIME	RH	REL WIND DIR & SPD	SHIPS HEAD & SPD	AITKEN CON	# PARTICLES / .28 L	>.3	>.6	>1.2	>3.0	>5.0
22 [illegible]	93	20 1	0 0	0	104567	30760	11984	15	0	
22 [illegible]	93	20 1	0 0	0	104660	31147	12517	15	0	
22 [illegible]	93	20 1	0 0	0	120771	36450	14258	20	0	
22 [illegible]	93	20 1	0 0	0	89714	22441	8413	6	0	
22 1015	93	20 1	0 0	0	96659	27913	10500	10	0	
22 1040	93	20 1	0 0	0	100800	26583	10641	8	0	
22 1130	93	20 1	0 0	0	104968	31062	12386	9	0	
22 1200	92	170 2	52 0	0	84874	24125	9211	3	0	
22 1300	90	45 3	104 9	0	90750	25340	9591	8	0	
22 1400	85	180 5	155 9	6400	114549	33457	12966	9	0	
22 1500	88	225 7	155 9	79000	37164	6476	2095	36	0	
22 1600	89	155 2	153 9	6200	14650	3333	1137	5	0	
22 1700	84	215 8	179 9	3100	26289	5464	1946	9	0	
22 1755	85	275 5	0 0	10500	17689	3778	1328	5	0	
22 1810	85	260 3	0 0	4000	9248	2949	1182	9	0	
22 1900	91	140 3	0 0	3800	10718	2870	1127	13	0	
22 1915	91	150 3	0 0	8100	11929	3114	1242	20	0	
22 1930	91	150 3	0 0	6000	12038	3151	1286	23	0	
22 1945	91	150 3	0 0	9300	12081	2964	1257	20	0	
22 1950	90	145 6	0 0	14000	12468	3145	1220	19	0	
22 2020	90	255 2	0 0	4400	15438	3562	1453	12	0	
22 2115	92	120 9	100 9	4300	14500	3471	1295	14	0	
22 2200	97	11515	100 9	10000	14504	3245	1251	10	0	
22 2300	89	13512	100 9	11500	11953	2697	1093	7	0	
23 0	87	13512	100 9	5100	11140	2751	1065	8	0	
23 100	87	13010	95 9	4200	13020	2710	918	6	0	
23 200	92	135 8	90 9	3800	33570	6770	2222	8	0	
23 235	92	160 2	0 0	5800	63264	14772	5139	10	0	
23 315	92	330 3	325 9	2900	63350	14540	5240	17	0	
23 400	92	340 4	324 9	4700	46733	10112	3350	5	0	
23 530	92	340 4	324 9	3600	38071	7335	2269	3	0	
23 600	92	325 3	300 9	0	29975	5441	1575	0	0	
23 700	92	310 2	300 9	0	35975	6897	2170	5	0	
23 800	89	315 3	290 9	0	32127	5870	1860	5	0	
23 900	80	345 2	315 9	0	22542	3820	1370	5	0	

DATE & TIME	RH	REL WIND DIR & SPD	SHIPS HEAD & SPD	AITKEN CON	# PARTICLES / .28 L	>.3	>.6	>1.2	>3.0	>5.0
23 1000	78	330 4	300 9	0		25258	4480	1253	5	0
23 1400	82	250 5	0 0	7300		18568	4242	1570	17	0
23 1500	85	215 8	215 5	2700		13656	3353	1327	21	0
23 1600	82	300 7	360 9	5100		16043	3679	1411	27	0
23 1650	86	265 8	0 0	8000		40053	9837	3524	17	0
23 1800	87	245 9	262 9	6400		76557	18645	6462	12	0
23 2000	88	250 1	0 0	3000		18165	4097	1571	18	0
23 2100	86	300 1	0 0	2800		20170	4800	1805	16	0
23 2200	90	330 1	0 0	3500		21142	4760	1852	21	0
23 2300	91	200 1	0 0	4100		22894	5540	2212	23	0
24 8	93	5 3	160 4	6000		26665	6232	2352	20	0
24 30	93	305 6	318 4	10800		34049	8019	3021	22	0
24 100	90	270 1	0 0	15500		75830	19535	7371	28	0
24 130	90	135 6	100 5	18000		66626	16280	6169	20	0
24 155	85	180 2	0 0	17500		31474	5770	2160	23	0
24 200	85	150 2	0 0	19500		36695	6711	2382	23	0
24 300	86	225 7	245 9	16000		35510	6150	2032	11	0
24 330	86	135 2	0 0	17500		45800	8344	2665	23	0
24 400	86	230 6	245 9	15500		49516	9750	3090	11	0
24 430	86	240 9	246 9	10000		34785	7334	2560	20	0
24 500	87	60 5	50 9	5000		43400	9248	3200	24	0
24 530	87	25 4	38 9	6900		46142	9792	3456	19	0
24 550	85	310 2	0 0	6200		62980	14200	5069	19	0
24 630	85	170 6	147 9	12000		55820	13200	4600	19	0
24 700	84	160 8	167 9	14000		49738	9260	3000	15	0
24 800	80	140 8	150 9	0		54937	10550	3285	14	0
24 830	80	140 8	150 9	0		37551	6447	2111	10	0
24 900	76	75 2	0 0	0		30717	5212	1866	10	0
24 930	76	75 2	0 0	0		32532	5742	1957	10	0
24 1000	77	320 8	325 9	0		41046	6916	2050	15	0
24 1030	77	320 8	325 9	0		63024	11004	3446	15	0
24 1100	77	32011	330 9	0		75771	16170	5225	15	0
24 1200	71	135 1	100 9	0		92097	26256	10170	30	0
25 2100	83	27011	245 1	3800		10826	2636	712	7	0
25 2230	83	285 6	305 1	3600		8264	3261	1161	18	0

DATE & TIME	RH	REL WIND DIR & SPD	SHIPS HEAD & SPD	AITKEN CON	# PARTICLES / .28 L	>.3	>.6	>1.2	>3.0	>5.0
25 2300	83	28010	0 0	0		9490	3630	1378	30	0
26 0	83	290 6	0 0	0		9317	3784	1531	40	0
26 100	87	45 1	0 0	0		9486	4147	1890	50	0
26 200	86	225 1	0 0	0		13584	5517	2390	40	0
26 300	90	240 1	0 0	0		10170	4661	2259	40	0
26 400	90	360 9	340 9	0		9960	4600	2300	40	0
26 500	86	300 2	0 0	10000		11768	5540	2600	51	0
26 600	91	270 6	270 9	5600		11050	5090	2650	47	0
26 700	86	275 5	297 9	3000		10505	4829	2394	55	1
26 800	86	315 9	295 9	4500		9229	4167	2088	26	0
26 900	86	30010	295 9	6000		14336	5851	2650	36	0
26 1000	85	30012	295 9	7300		14455	6019	2791	36	0
26 1100	81	30012	295 9	12200		11144	4776	2256	24	0
26 1200	82	29017	295 9	10500		10352	4365	1975	19	0
26 1300	81	29016	284 9	9600		10857	4545	2059	12	0
26 1400	77	27017	278 9	5600		10953	4605	2077	15	0
26 1500	77	24514	0 0	5400		12162	5280	2464	21	0
26 1600	71	23512	278 8	4400		11940	5086	2280	15	0
26 1700	52	29021	278 8	20000		7640	2942	1205	26	0
26 1800	60	30514	70 0	7800		5229	1917	850	55	0
26 2100	51	32512	70 3	0		5391	1320	520	25	0
26 2200	62	325 8	80 3	0		4700	1446	573	25	0
26 2300	62	325 4	80 3	0		3186	1067	452	15	0
27 0	73	150 3	90 2	7300		9089	2654	1097	26	0
27 104	95	130 4	0 0	10000		7280	3094	1506	45	0
27 119	95	115 3	0 0	8400		6134	2455	1215	23	0
27 145	94	200 2	0 0	7600		6321	2358	1047	24	0
27 200	93	210 1	0 0	7000		7694	3097	1384	23	0
27 212	92	235 8	253 4	5800		9576	3850	1682	24	0
27 223	82	240 1	0 0	6800		10586	4300	1849	25	0
27 250	82	240 1	0 0	7100		10122	4147	1820	25	0
27 306	84	315 1	0 0	6700		10260	4209	1890	23	0
27 324	85	310 1	0 0	16000		10808	4253	1851	26	0
27 339	90	310 1	0 0	52000		10212	3996	1650	15	0
27 356	90	310 1	0 0	23000		10383	4025	1807	40	0

DATE & TIME	RH	REL WIND DIR & SPD	SHIPS HEAD & SPD	AITKEN CON	# PARTICLES / .28 L	>.3	>.6	>1.2	>3.0	>5.0
27 417	SC	30 1	0 0	35000		10864	4320	1530	35	0
27 44C	SC	8C 1	0 0	23500		12414	4915	2272	34	0
27 5CC	ES	27S 4	0 0	0		9864	4105	1908	25	0
27 6CC	80	270 2	0 0	0		9689	4014	1958	15	0
27 7CC	75	25S 2	0 0	0		12690	4986	2504	25	0

REFERENCES

1. Blifford, I. H., 1970: "Tropospheric Aerosols", J. Geophys. Res., 75, 3099-3103.

2. Businger, J. A., J. C. Wyngaard, Y. Izumi, and E. F. Bradley, 1971: "Flux-Profile Relationships in the Atmospheric Surface Layer," J. Atmos. Sci., 28, 181-189.

3. Day, J. A., 1964: "Production of Droplets and Salt Nuclei by the Bursting of Air-Bubble Films," Q. J. Roy. Meteor. Soc., 90, 72-78.

4. Ericksson, E., 1959: "The Yearly Circulation of Chloride and Sulphur in Nature; Meteorological, Geochemical and Pedological Implications," Tellus, 11, 375-403.

5. Fairall, C. W., K. L. Davidson, J. Houlihan, and G. E. Schacher, 1977: Turbulence and Drag Coefficient over the Ocean. Unpublished, Environmental Physics Group, Naval Postgraduate School, Monterey, California, 19 pp.

6. Fitzgerald, J. W., 1975: "Approximation Formulas for the Equilibrium Size of an Aerosol Particle as a Function of its Dry Size and Composition and the Ambient Relative Humidity," J. Appl. Meteorol., 14, 1044-1049.

7. Fitzgerald, J. W. and R. E.Ruskin, 1977: A Marine Aerosol Model for the North Atlantic, Naval Research Laboratory Memorandum Report 3430, Washington, D. C., 104-110.

8. Friedlander, S. K., 1961: "Theoretical Considerations for the Particle Size Spectrum of the Stratospheric Aerosol," J. Meteorol., 18, 753-759.

9. Hidy, G. M., P. K. Mueller, H. H. Wang, J. Karney, S. Twiss, M. Imada, and A. Alcocer, 1974: "Observations of Aerosols over Southern California Coastal Waters," J. Appl. Meteorol., 13, 96-106.

10. Junge, C. E., 1972: "Our Knowledge of the Physico-Chemistry of the Undisturbed Marine Environment," J. Geophys. Res., 77, 5183-5200.

11. Junge, C. E. and R. Jaenicke, 1971: "New Results in Background Aerosols Studies from the Atlantic Expedition of the R. V. Meteor, Spring, 1969," Aerosol Sci., 2, 305-314.

12. Kientzler, C. F., A. B. Arons, D. C. Blanchard, and A. H. Woodcock, 1954: "Photographic Investigation of the Projection of Droplets by Bubbles Bursting at a Water Surface," Tellus, 6, 1-7.

13. Lieberman, A., and R. J. Allen, 1969: Theoretical and Experimental Light Scattering Data for a Near Forward System. Presented at American Association for Contamination Control, May 19-22, 15 pp.

14. Lovett, R. F., 1975: The Occurrence of Airborne Sea Salt and its Meteorological Dependence. M. S. Thesis, Heriot-Watt University, United Kingdom, 194 pp.

15. Lumley, J. L. and H. A. Panofsky, 1964: The Structure of Atmospheric Turbulence, Interscience Publishers, John Wiley and Sons, London, 239 pp.

16. Mack, E. J., 1977: Measurements of Aerosol Characteristics in the Marine Boundary Layer along the Offshore Margin of Southern California, Calspan Corp., Buffalo, N.Y., Prepared For: Naval Postgraduate School, Monterey, California, 44 pp.

17. Mack, E. J. and U. Katz, 1977: Measurements of Aerosol and Micrometeorological Characteristics of the Marine Boundary Layer in the Gulf of Mexico, Calspan Corp., Buffalo, N.Y., Prepared For: Naval Avionics Facility, Indianapolis, Indiana, 58 pp.

18. Mason, B. J., 1954: "Bursting of Air Bubbles at the Surface of Sea Water," Nature, 174, 470-471.

19. Mason, B. J., 1975: Clouds, Rain and Rainmaking, Cambridge University Press, Cambridge, 189 pp.

20. Meszaros, A. and K. Vissy, 1974: "Concentration, Size Distribution and Chemical Nature of Atmospheric Aerosol Particles in Remote Oceanic Areas," Aerosol Sci., 5, 101-109.

21. Monahan, E. C., 1968: "Sea Spray as a Function of Low Elevation Wind Speed," J. Geophys. Res., 73, 1127-1137.

22. Monin, A. S. and A. M. Obukhov, 1954: "Basic Laws of Turbulent Mixing in the Ground Layer of the Atmosphere," Akademiia Navk SSSR, Leningrad, Geofizicheskii Institut, Trudy No. 24 (151), 163-187, English Translation by Miller, J., 1959.

23. Moore, D. J., 1952: "Measurements of Condensation Nuclei over the North Atlantic," Q. J. Roy. Meteor. Soc., 78, 596-602.

24. Moore, D. J. and B. J. Mason, 1954: "The Concentration, Size Distribution and Production Rate of Large Salt Nuclei over the Oceans," Q. J. Roy. Meteor. Soc., 80, 583-590.

25. Panofsky, H.A., 1969: "Air Pollution Meteorology," American Scientist, 57, 269-285.

26. Panofsky, H. A., A. K. Blackadar, and G. G. McVehil, 1960: "The Diabatic Wind Profile," Q. J. Roy. Meteor. Soc., 86, 390-398.

27. Paterson, M. P. and K. T. Spillane, 1969: "Surface Films and the Production of Sea-Salt Aerosol," Q. J. Roy. Meteor. Soc., 95, 526-534.

28. Ruskin, R. E., R. K. Jeck, and H. E. Gerber, 1976: Progress Report on Sea Salt Measurement September 1975 - January 1976, Naval Research Laboratory Memorandum Report 3270, Washington, D. C., 10 pp.

29. Toba, Y., 1965a: "On the Giant Sea-Salt Particles in the Atmosphere, 1, General Features of the Distribution," Tellus, 17, 131-145.

30. Toba, Y., 1965b: "On the Giant Sea-Salt Particles in the Atmosphere, 2, Theory of the Vertical Distribution in the 10-m Layer over the Ocean," Tellus, 17, 365-382.

31. Whitby, K. T. and B. Y. Liu, 1973: Advances in Instrumentation and Techniques for Aerosol Generation and Measurement, P. L. Pub. No. 216, University of Minnesota, 34 pp.

32. Winkler, P., 1973: "The Growth of Atmospheric Aerosol Particles as a Function of the Relative Humidity---II. An Improved Concept of Mixed Nuclei," Aerosol Sci., 4, 373-387.

33. Woodcock, A. H., 1953: "Salt Nuclei in Marine Air as a Function of Altitude and Wind Force," J. Meteorol., 10, 362-371.

34. Woodcock, A. H., 1972: "Smaller Salt Particles in Oceanic Air and Bubble Behavior in the Sea," J. Geophys. Res., 77, 5316-5321.

35. Wyngaard, J. C., Y. Szumi, and S. A. Collins, 1971: "Behavior of the Refractive Index Structure Parameter near the Ground," Jour. Opt. Soc. America, 61, 1646-1650.

36. Zinky, W. R., 1962: "A New Tool for Air Pollution Control: The Aerosol Particle Counter," J. Air Pollution Control Assoc., 12, 578-583.

INITIAL DISTRIBUTION LIST

		No. Copies
1.	Defense Documentation Center Cameron Station Alexandria, Virginia 22314	2
2.	Library, Code 0142 Naval Postgraduate School Monterey, California 93940	2
3.	Department of Meteorology Library, Code 63 Naval Postgraduate School Monterey, California 93940	1
4.	Prof. Kenneth L. Davidson, Code 63Ds Department of Meteorology Naval Postgraduate School Monterey, California 93940	9
5.	Prof. Gordon E. Schacher Department of Physics and Chemistry Naval Postgraduate School Monterey, California 93940	2
6.	Mr. Steve Rinard, Code 63 Department of Meteorology Naval Postgraduate School Monterey, California 93940	1
7.	Mr. Eugene J. Mack Calspan Corporation P. O. Box 235 Buffalo, New York 14221	1
8.	Captain Harry Hughes AFIT/CIPF Wright-Patterson AFB, Ohio 45433	2
9.	Air Weather Service AWS/TF Scott AFB, Illinois 62225	1
10.	Captain Valente Macias, Jr. 3805 Mt. Rainier, Northeast Albuquerque, New Mexico 87111	1
11.	Captain Alan A. Simoncic PSC #2, Box 2471 Hickam AFB, Hawaii 96853	5

Thesis
S49455
c.1
Simoncic
A comparative study
of the coastal marine
aerosol.